Study of time reversal violation in β decay of polarized ^{8}Li

J. Sromicki, M. Allet,* K. Bodek,† W. Hajdas,‡ J. Lang, R. Müller, S. Navert, O. Naviliat-Cuncic, and J. Zejma§
Institut für Teilchenphysik, Eidgenössische Technische Hochschule Zürich, CH-8093 Zürich, Switzerland

W. Haeberli
Department of Physics, University of Wisconsin, Madison, Wisconsin 53706
(Received 19 May 1995)

The transverse polarization in a plane perpendicular to the nuclear spin axis has been determined for electrons emitted in the β decay of polarized ^{8}Li. Such a spin component signals a violation of time reversal symmetry. Using a sample of ^{8}Li nuclei with vector polarization of ~ 0.11 and a polarimeter with average analyzing power $S=-0.10$, the asymmetry in the Mott scattering of decay electrons was measured with an accuracy of $\pm 4\times 10^{-5}$. From the asymmetry, the transverse spin polarization of the electrons has been determined with an accuracy of $\pm 4\times 10^{-4}$, and the amplitude $R=(-0.2\pm 4.0)\times 10^{-3}$ of the triple correlation between nuclear spin, momentum, and spin of the electron has been obtained. These results represent the most precise measurement of the transverse polarization of leptons emitted in weak decays. Time reversal violating part of the correlation amplitude, $R_{\mathrm{TRV}}=(-0.9\pm 4.0)\times 10^{-3}$, is deduced. It provides the first direct determination of the imaginary, charged weak tensor interaction $-0.022<\mathrm{Im}(C_T+C_T')/C_A<0.017$ or alternatively $-0.004<\mathrm{Im}(a_{RL}^T)<0.005$ (90% C.L.). These are the tightest limits for exotic (nonvector or axial vector) time reversal violating couplings in semileptonic weak decays. A report is presented with emphasis on experimental details and data analysis. Relations of this study to other tests of time reversal violation are discussed.

PACS number(s): 24.80.+y, 23.40.Bw, 13.88.+e, 13.30.Ce

I. INTRODUCTION

The CPT theorem [1] links time reversal symmetry T with a combination of particle-antiparticle and parity symmetries (CP). This grand theoretical conjecture and experimental evidence supporting it [2] give rise to expectations that T violation should be accompanied by a corresponding CP violation and vice versa.

The existence of CP violation in the decay of neutral kaons is firmly established: in a number of experiments, the observed effects exceed the statistical uncertainties by more than an order of magnitude. The startling discovery of the CP violation phenomena has prompted vigorous theoretical activity. The best known mechanisms considered as sources of CP violation are the superweak interaction [3], Cabibbo-Kobayashi-Maskawa (CKM) mixing of the quark states [4], a θ term in the QCD Lagrangian [5], models involving left- and right-handed gauge bosons [6], multiplets of Higgs particles [7], or leptoquarks [8]. The CKM mixing and the θ interaction term are embedded into the standard model (SM) of particles and their interactions. The former mechanism is particularly important, since it is the only one that arises within a context of already known physics. CP violation in the CKM frame arises as a genuine phenomenon of weak interactions with a subtle interplay of all three quark families. This model predicts sizable CP violation effects in processes involving heavy quarks. Its predictions for the systems built of the lightest quarks, d and u, are very low, and in fact inaccessible to a test by the present generation of laboratory experiments.

Another, though indirect evidence of CP or T violation, is an excess of matter over antimatter in the present Universe. With perfect CP or T invariance, all the baryons and antibaryons created in the big bang explosion would have annihilated and the present world would be filled mostly with energy in the form of massless quanta of radiation [9]. It was pointed out [10] that, beside baryon number violating processes, the violation of CP or T symmetry is one of the *necessary* conditions to produce an excess of baryons over antibaryons.

Experimental evidence, particularly the absence of characteristic annihilation radiation, suggests that even the largest structures in the Universe are composed of regular matter. However, the CP violating interaction, detected in the kaon system and incorporated into the SM, is *too weak* to produce so much matter in the baryogenesis process [11]. Therefore cosmology provides a hint that there exist also *other mechanisms* that break CP or T invariance. In contrast to the CKM model, sizable effects for systems built of light quarks could suggest a more natural explanation of the large baryon/antibaryon asymmetry.

There is a general consensus that an observation of CP or T symmetry breaking outside the kaon system may provide a clue for a new view on particles or their interactions. Motivated by the *contradictions* between the SM and cosmology we have performed a test of time reversal symmetry.

*Present address: Alusuisse, Schweizerische Aluminium AG Siders, 3965 Chippis, Switzerland.
†On leave from Jagellonian University, Cracow, Poland.
‡Present address: Paul Scherrer Institut, 5232 Villigen, Switzerland.
§Present address: Institute of Physics, Jagellonian University, 30059 Cracow, Poland.

II. STATUS OF T VIOLATION

A. Experiments and their implications

In the following survey of the most important experiments we emphasize that various studies of the two related discrete symmetries provide complementary information. The experiments in subfields of particle and nuclear physics are usually sensitive to different mechanisms of the CP or T violation.

CP forbidden processes, $\sim 2\times 10^{-3}$ in the branching ratios [12], have been observed in hadronic decays ($K^0\rightarrow \pi^+\pi^-$) and in semileptonic decays ($K^0\rightarrow \pi^\pm e^\mp \bar{\nu}$) of neutral kaons [2]. In recent years enormous efforts have been concentrated on the kaon experiments. The motivation for this generation of experiments was the theoretical discovery of a signature that may distinguish between the CKM and the superweak models of CP violation. An unavoidable consequence [13] of the CKM model is the mechanism of ''direct'' CP violation that leads to a strangeness-changing ($\Delta S=1$) transition in the decay amplitude. In contrast, the superweak interaction may change strangeness only by two units ($\Delta S=2$). Recent experimental reports from Fermilab [14] do not provide conclusive data in support of ''direct'' CP violation, although the earlier CERN data [15] have been considered as evidence against the superweak model. Though it is not related to the problem of ''direct'' CP violation, we note an observation of CP violation in a new decay channel where two charged pions are accompanied by a photon [16].

Direct determination of the time reversal violating part of the interaction in the kaon system is interesting in the context of our work. A thorough analysis of the classic kaon decay experiments, which leads to the conclusion that '' . . . the CPT violating interaction strength is at most a few percent of the CPT conserving, T violating interaction . . . '' is presented in the textbook [17]. Recent study searches for T violation effects using a new experimental approach [18].

Recent theoretical findings [19] suggest that kaon experiments alone cannot distinguish between the two models. It is expected that CP violation phenomena will be exhibited in a system of neutral B mesons [20]. However, it was pointed out [21] that the parameters describing CP violation in heavy quark systems lie in an area that will make a selection between the superweak and the CKM model particularly difficult, even in the case of positive evidence of CP violation from B meson experiments.

Not only decay processes, but also static properties of particles may be influenced by CP or T noninvariant interactions. The best known example is the electric dipole moment (EDM). Nonzero EDM's are not present at the Lagrangian level in fundamental, renormalizable field theories [22]. They may be, nevertheless, induced by parity *and* time reversal violating interactions via higher order processes (quantum loop corrections). For example, a third order calculation in the CKM frame is required to produce a nonvanishing EDM for quarks and electrons [23]. The most elaborate search for a permanent EDM is performed with polarized ultracold neutrons. The results of the two leading experiments [24] are interpreted as an upper limit of $1.2\times 10^{-25} e$ cm (95% C.L.) for the EDM of the neutron [25]. This limit is impressively small. Recently, even tighter constraints on the EDM's of the neutron and electron have been provided by experiments with more complex systems, notably Hg and Tl atoms [24]. EDM experiments restrict the θ interaction term, which may arise in the QCD sector of the standard model, to $\sim 10^{-9}$ of its natural strength [22]; no other experiments are better suited for search of T violation generated by strong interaction. EDM predictions based on the CKM mechanism are still ~ 7 orders of magnitude lower [26] than the experimental determinations. The exact values of these predictions vary by large factors, depending on the details of the assumptions used in the calculations. The predicted effects are in general so small that it seems unrealistic to expect that the EDM experiments with ultracold neutrons will soon shed light on details of T violation generated by the CKM scheme [26]. Other interesting mechanisms of T violation, like multiple Higgs bosons, or left-right symmetric models, allow an EDM of the neutron only 1–2 orders of magnitude smaller than the present experimental limit [26]. Their effects may be tested therefore by the next generation of EDM experiments.

The obvious way to study time reversal symmetry is to compare a certain physical process and *the same* process running backwards in time. This leads to the principle of detailed balance, which is based on the invariance of the scattering matrix S under time reversal transformation T [27]. Detailed balance was tested in cross sections [28] and in polarization observables [29] for a number of nuclear reactions. The results show that T-violating amplitudes are at most 10^{-3} to 10^{-2} of the dominating strong interaction amplitudes. New prospects for T violation experiments with strongly interacting systems have appeared following a discovery of large enhancement factors of 10^3-10^6 for parity nonconserving phenomena in the interaction of polarized neutrons with nuclear media. It is argued [30] that similar amplification mechanisms may operate for effects of T violation. An experiment along these lines is in preparation [30]. Though an interpretation of these experiments in terms of statistical models is not free of controversy, and conjectured enhancement factors are not large enough to probe the interaction scale involved in kaon experiments, an unambiguous signal of T-odd effects in nuclear reactions would be a very important discovery.

Experiments with γ decays avoid some uncertainties associated with strong nuclear forces. These experiments search for T-odd components in the nuclear wave functions or electromagnetic transition operators. Since electromagnetic interactions are parity conserving, P-even observables are studied in tests of time reversal symmetry. Observables that are P even but T odd are formed by proper combinations of the momenta and polarizations of the involved nuclei and γ rays. Here, a limit of $\sim 10^{-3}$ is set on the strength of a P conserving but T violating force with respect to electromagnetic forces [31]. γ decay experiments probe a domain that has eluded other searches for T violation. However, once again an interaction scale that is much stronger than weak interactions is investigated. For P-odd components of a T violating interaction, experiments with electromagnetic decays are not capable of providing meaningful sensitive limits.

Our study belongs to the class of experiments which determine correlations between polarizations and momenta of particles involved in weak decays. The lowest order T-odd

TABLE I. The results (in 10^{-3} units) of the experiments searching for time reversal violation in triple correlations in weak decays: J is the spin of the decaying system, p is the momentum of the decay product, and σ is the spin of the emitted lepton. Self-explanatory subscripts are used to associate (pseudo)vectors with the particles.

T violating and P conserving correlations			
Decay	Correlation	Result	Ref.
$\vec{n}\to pe^-\bar{\nu}_e$	$\vec{J}_n(\vec{p}_e\times\vec{p}_p)$	-1.1 ± 1.7	ILL [32]
$\vec{n}\to pe^-\bar{\nu}_e$	$\vec{J}_n(\vec{p}_e\times\vec{p}_p)$	-2.7 ± 3.3	LNPI [33]
$^{19}\vec{\text{Ne}}\to{}^{19}\text{F}e^+\nu_e$	$\vec{J}_{\text{Ne}}(\vec{p}_{\text{F}}\times\vec{p}_e)$	0.1 ± 0.6	PU [34]
$K^+\to\vec{\mu}^+\pi^0\nu_\mu$	$\vec{p}_\mu(\vec{p}_\pi\times\vec{\sigma}_\mu)$	-3 ± 5	BNL [35]
$K^0\to\vec{\mu}^+\pi^-\nu_\mu$	$\vec{p}_\mu(\vec{p}_\pi\times\vec{\sigma}_\mu)$	2 ± 6	BNL [36]
$\vec{\Sigma}^-\to ne^-\bar{\nu}_e$	$\vec{J}_\Sigma(\vec{p}_n\times\vec{p}_e)$	110 ± 100	FNAL [37]
T violating and P violating correlations			
Decay	Correlation	Result	Ref.
$^{19}\vec{\text{Ne}}\to{}^{19}\text{F}\vec{e}^+\nu_e$	$\vec{J}_{\text{Ne}}(\vec{p}_e\times\vec{\sigma}_e)$	-79 ± 53	PU [38]
$\vec{\Lambda}^0\to\pi^-\vec{p}$	$\vec{J}_\Lambda(\vec{p}_p\times\vec{\sigma}_p)$	-100 ± 70	BNL [39]
$\vec{\Lambda}^0\to\pi^-\vec{p}$	$\vec{J}_\Lambda(\vec{p}_p\times\vec{\sigma}_p)$	-94 ± 60	CERN [40]
$\vec{\mu}^+\to\vec{e}^+\nu_e\bar{\nu}_\mu$	$\vec{J}_\mu(\vec{p}_e\times\vec{\sigma}_e)$	7 ± 23	SIN [41]
$^8\vec{\text{Li}}\to{}^8\text{Be}\vec{e}^-\bar{\nu}_e$	$\vec{J}_{\text{Li}}(\vec{p}_e\times\vec{\sigma}_e)$	-0.2 ± 4.0	This work

combination of vectors and pseudovectors available in the decay process appears in the form of their triple product. Here we distinguish the one spin–two momenta correlation from the one that involves two spins and one momentum. The former is P even while the latter is P odd, and even if they are determined for the same decay process, they bear sensitivity to different aspects of T violation. Study of P-odd observables in weak decays is meaningful, since parity is anyway maximally violated in these processes, and therefore it does not bring additional constraints. Here, we present a summary of the most precise experimental results for triple correlations in weak interactions. A detailed discussion of the implications that are related to our study will follow at the end of this paper.

The upper part of Table I presents the results of the experiments measuring T-odd, P-even correlations. These observables have been studied for the neutron [32,33], ^{19}Ne [34], K^+ [35], K^0 [36], and Σ^- [37] decays. T-odd, P-odd correlations have been measured prior to our experiment for ^{19}Ne [38], Λ^0 [39,40], and μ^+ [41] decays; the results are shown in the lower part of Table I.

We note that determinations of P-odd components of the T violating interaction are roughly one order of magnitude less precise. The reason is the necessity to establish the spin direction of the decay product. Such a measurement is usually more difficult than the determination of the direction of the emitted particle. Since the two types of correlations provide independent information on the mechanism of T violation, improvement in precision for P odd observables is very desirable.

A new generation of triple correlation experiments is in preparation (e.g., neutron decay, or K decay [42]) with the goal of improving the accuracies by factors of ~5. Once again, the more easily accessible P-even correlations will be studied. To our knowledge, none of the performed or planned experiments are sensitive enough to disclose the tiny correlation effects which are generated by the standard model. Their motivation is rather to use time reversal violation as a tool to search for "physics beyond the standard model."

B. Arguments for tests with β decay

The vector-axial vector (V-A) [43] form of the semileptonic weak interaction is embedded in the standard model by *assuming* that $W^\pm$ and Z^0 bosons with their purely left-handed couplings are the *only* mediators of the weak force. The standard model does not predict sizable time reversal violating phenomena for systems built of the lightest, u and d, quarks.

In contrast to a popular belief that the interaction responsible for β decay has a strict V-A structure with real, T-conserving couplings, there is still room for sizable deviations from the standard theory. Such deviations may be caused by admixtures of exotic scalar and tensor interaction terms that are allowed by Lorentz invariance [44]. In fact, model independent constraints on the strength of the imaginary scalar and tensor couplings are up to ~0.1 of the regular V-A amplitude [45]. Below we discuss arguments for performing a new test of T violation in β decay, with particular focus on the tensor interaction.

(1) Precise experimental verification of the V-A ansatz is of utmost importance. The absence of T violation effects in the frame of the standard model is a favorable situation in a search for new phenomena.

(2) A well developed theory and phenomenology provides a convenient framework for the interpretation of a wide class of experiments. The results obtained with various nuclei and observables are related via the weak interaction coupling constants. Useful limits for these couplings are obtained also in case of not finding a time reversal violating signal.

(3) Some available models, based, e.g., on Higgs boson or leptoquark exchange, admit fundamental scalar *and* tensor interactions. Contrary to a general conviction, such a tensor contribution *may* be generated within a framework of renormalizable field theory, e.g., via a Fierz rearrangement of the gauge interaction defined in the leptoquark picture [8,44].[1]

(4) Recently reported inconsistencies in the pion radiative decay data [46] point to a $\sim4\times10^{-2}$ tensor amplitude. Although the experimental situation should be clarified, these data have triggered serious discussions concerning a tensor interaction [47].

(5) The real part of the tensor couplings is restricted to few parts per thousand of the regular weak amplitude by measurements of the Fierz interference term b in ^{22}Na decay (Ref. [45] and references therein). Large room is left for the time reversal violating, imaginary tensor couplings; in fact, no dedicated study of this aspect of the weak interaction has been performed up to now.

Our measurement of the transverse polarization for electrons emitted in the β decay of polarized ^{8}Li is a first direct

[1]It should be also noted that gravity *is* a tensor interaction and undeniably *exists*, despite problems with formulating it within a renormalizable gauge theory.

determination of the time reversal violating tensor terms. The first results of this experiment have been published in [48]. Here, we present a complete account, with particular emphasis on the experimental details and data analysis. The bulk of data ($\sim$90%) was collected after our first publication, therefore technicalities will refer mostly to the last series of measurements that have led to a fourfold improvement in the accuracy.

III. EXPERIMENT

It was noticed by Lee and Yang on the occasion of their discovery of parity violation [49] that the decay rate, in a weak process governed by a Lorentz invariant Hamiltonian with a point interaction between the involved fermions, depends in a simple manner on the geometric arrangement of the vectors and pseudovectors characterizing the emitted particles. This observation was soon generalized to more complicated experimental situations. Jackson *et al.*, in a series of classical papers [50], have derived expressions for the angular distributions of the energies and polarizations of leptons emitted in the β decay from polarized nuclei.

Restricting the formulas to terms that are important in searches for time reversal violation we obtain a distribution function W, which describes correlations between the nuclear polarization $\vec{J}$, the polarization of the electron $\vec{\sigma}$, and the momenta of the electron $\vec{p}$ and neutrino $\vec{p}_\nu$ [50]:

$$W \propto \left(1 + A\frac{\vec{J}\vec{p}}{E} + D\frac{\vec{J}(\vec{p}\times\vec{p}_\nu)}{EE_\nu} + R\frac{\vec{J}(\vec{p}\times\vec{\sigma})}{E} \right).$$

Here A is the parity violating β decay asymmetry parameter, the D and R coefficients denote the amplitudes of the time reversal violating P even, T odd, and P,T odd correlations that were discussed in the preceding section, and E,E_ν are the total energies of the electron and the neutrino, respectively. We use units with the velocity of light $c=1$. A Lorentz invariant theory with point interactions between particles predicts a simple $p/E=v$ dependence of the rate modulations on the velocity v. This dependence is explicitly disclosed in the formulas, so that the coefficients $A,D,R,\ldots$ are energy independent.

The decay parameters A, D, and R, depend on the Fermi M_F and Gamow-Teller $M_{\rm GT}$ nuclear matrix elements and on the weak interaction coupling constants. The matrix elements take into account the nuclear structure of the states involved in the transition, while the coupling constants describe genuine effects of the weak interactions. A detailed discussion will follow in Sec. VII. Jackson *et al.* have also considered an additive correction term to the correlation parameters, due to the electromagnetic final state interactions (FSI). We note that the FSI contribution to the R correlation is proportional to the decay asymmetry parameter A [50]:

$$R_{\rm FSI} = -\frac{\alpha Z m}{p} A,$$

where α is the fine structure constant, Z is the charge of the residual nucleus, and m,p are the electron mass and momentum. The FSI terms for the R correlation are naturally suppressed in the decays of light nuclei with high energy release. This correction may also be very small for transitions with an exceptionally small asymmetry parameter A.

A. ^{8}Li nucleus

1. Advantages

The ^{8}Li nucleus offers some advantages for an R correlation experiment.

(1) Final state effects are extraordinarily small due to the low nuclear charge of the recoil nucleus ($Z=4$) and the high decay energy ($E_{\rm max}=13.1$ MeV). It is worth noting that the $R_{\rm FSI}$ correction for ^{8}Li decay is probably the smallest for all β unstable nuclei, including the neutron.

(2) The transverse polarization of the electrons with energies in the MeV range can be analyzed by Mott scattering from nuclei with a large charge. Appreciable analyzing powers (-0.1 to -0.4) are observed at large scattering angles, where the cross sections are however low.[2]

(3) Polarized ^{8}Li nuclei may be produced in the polarization transfer reaction $^7{\rm Li}(\vec{d},p)^8\vec{\rm Li}$. Fast reversal of the nuclear polarization is achieved by reversing the spin of the deuterons. This is of primary importance for the cancellation of systematic effects associated with efficiencies of the detectors, slow drifts in the amplification, etc.

(4) Low magnetic holding fields ($\sim$ 2 mT only) maintain the nuclear polarization for periods longer than the half life of the decay in isotopically pure ^{7}Li host targets. Such targets provide a high yield of decay electrons and a low background radiation.

(5) The high energy of the emitted electrons brings an advantage in discrimination against usually low energy background radiation.

2. Decay characteristics

The ^{8}Li nucleus, in its ground state, is a member of the isospin triplet (^{8}Li, ^{8}Be, ^{8}B). It decays to the 1.5 MeV broad excited state of ^{8}Be, with a centroid at 2.9 MeV above the threshold in the α-α system. The most important data for this decay are shown in Fig. 1. A low value of the comparative lifetime logft = 5.4 [51], and good agreement of the energy spectra of the emitted electrons with the phase space predictions [52] assure that we are dealing with an allowed β decay. Accordingly, the formalism of Ref. [50] is applicable.

The transition $^8{\rm Li} \rightarrow {}^8{\rm Be}$ is dominated by the Gamow-Teller strength, which eliminates nuclear structure uncertainties in the interpretation of the results (Sec. VII).

B. Source of polarized ^{8}Li

1. Beam and time structure of the measurements

Polarized ^{8}Li nuclei were produced by polarization transfer in the reaction $^7{\rm Li}(\vec{d},p)^8\vec{\rm Li}$ initiated by 10 MeV deuterons provided by the PSI Injector Cyclotron.

[2] In the context of this class of experiments, it is unfortunate that a complete separation of spin states in a Stern-Gerlach experiment cannot be achieved for a free charged particle with a g factor of 2.

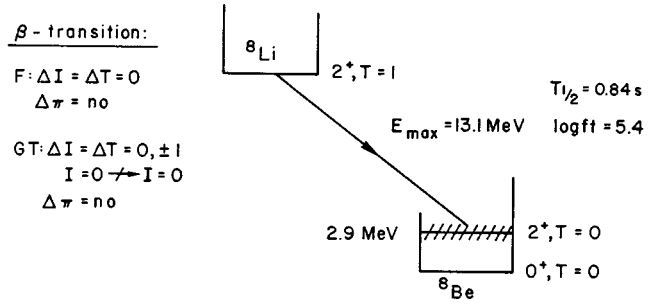

FIG. 1. Important data concerning ^{8}Li decay.

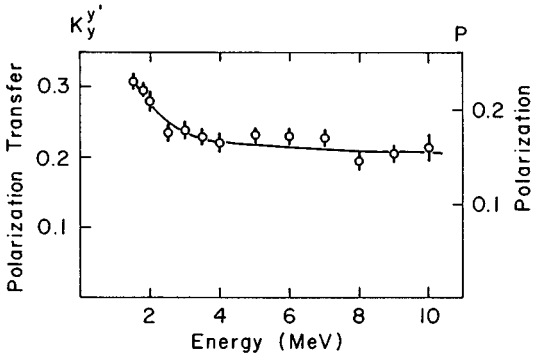

FIG. 2. Polarization transfer for the ^{7}Li$(\vec{d},p)^{8}\vec{\text{Li}}$ reaction. Left scale: polarization transfer coefficient $K_y^{y'}$ for a deuteron beam stopped in a thick target. Right scale: polarization of the ^{8}Li nuclei at the moment of their production obtained with a deuteron beam with a vector polarization $p_y = 0.5$.

The choice of energy was influenced by several factors. The transfer of the transverse polarization from the deuterons to the ^{8}Li nuclei, which was investigated in our earlier experiments [53], exhibits rather weak energy dependence (Fig. 2). Higher beam energies are preferable, since they provide larger production rates. Also, the extraction and acceleration of the beam are easier at higher energies. The most important argument for lower energies was an absence of reactions that might produce other than ^{8}Li β activity in the target.

The beam current used in the recent investigations was 1.5 μA compared to 0.4 μA in the earlier experiments [48]. This resulted in a very large decay rate of $\sim 2\times 10^{9}$ s^{-1}. The beam spot and the size of the ^{8}Li source were defined by 2 mm$\times$ 6 mm tantalum slits placed 40 mm from the target. Under our operating conditions $\sim$5% of the beam intensity was deposited on the slits.

The polarization of the beam was adjusted at the beginning of each series of measurements by tuning the radio frequency transitions at the ion source. The beam polarization was measured in the reaction ^{12}C$(\vec{d},p)^{13}$C. By using two groups of states of the residual nucleus we could determine simultaneously the vector and tensor polarization of the deuterons. Precise values of the vector and tensor analyzing powers (± 0.01) on a fine energy$\times$angle grid around 10 MeV and 90° were obtained in a separate experiment at the University of Wisconsin EN tandem accelerator. The beam polarization was checked periodically during the measurements. In accordance with our experience from other experiments, the polarization of the beam delivered from the ion source was stable on the level of 2% over a period of few days. A typical vector polarization of the deuteron beam was 0.53 ± 0.02, where the uncertainty quoted describes variations between different measuring periods. This figure is 80% of the maximum available vector polarization for a beam of spin-one particles without tensor polarization. Measured tensor moments of the beam were less than 0.03. They do not influence our results since the tensor polarization does not distinguish the direction of the polarization axis. In addition, transfer of the tensor polarization in the ^{7}Li $(d,p)^{8}$Li reaction is very low [54].

The measurements were performed in a cyclic fashion with a 0.33 s irradiation period of the target and a 1 s counting interval. During the counting period the beam was electrostatically deflected at the ion source. The counting interval was subdivided into 32 consecutive time bins. After five such activation/measurement cycles the beam polarization was reversed by switching radio frequency transitions at the ion source. In this way a fast spin reversal (every 7 s) of the ^{8}Li nuclei was achieved. Figure 3 shows the time structure of the measurement.

In order to avoid acquisition of events from remaining nuclei with ''wrong'' polarization, which have survived from the previous activation cycle, the data corresponding to the first irradiation after polarization reversal were not collected.

2. ^{7}Li target and ^{8}Li source polarization

The target, an isotopically pure 5 mm diameter ^{7}Li rod, was placed in a 7 mT magnetic field and cooled to liquid nitrogen temperature to preserve the polarization of the ^{8}Li nuclei for periods of time much longer than a half life of the decay.

The polarization of the ^{8}Li source was monitored continuously during the measurements with detectors mounted at 45° and 135° with respect to the vertical polarization axis. Energy and decay time spectra measured by the monitor detectors are shown in Fig. 2 in Ref. [48]. These detectors measure the up/down asymmetry in the decay rate of electrons, arising from parity violating β decay. In the approximation of a pure Gamow-Teller allowed transition, the asymmetry parameter for the ^{8}Li decay is $A=-1/3$ [50]. Small corrections were applied for the energy dependence of the asymmetry. Taking into account minor discrepancies between experimental data concerning the energy dependence [55], we estimate that the relative uncertainty in the absolute value of the target polarization is below 5%. This propagates as an uncertainty of the scale factor into our final result.

The mean polarization of the ^{8}Li source over the measuring period was between 0.11 and 0.12, depending on the condition of the target. Statistical errors in monitoring the target polarization are negligible. A typical development of the target polarization over a few days measuring period is shown in Fig. 4.

The observed long term drifts in the target polarization, $\sim \pm 0.005$/day, were caused most probably by the deterioration of the thermal contact between the ^{7}Li rod and its cool-

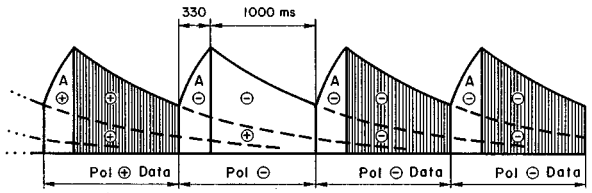

FIG. 3. Time structure of the measurement: activation periods are denoted by A, shaded areas correspond to counting intervals. Note that in order to increase the effective polarization of the ^{8}Li target we did not collect the data produced right after polarization reversal (second cycle in the drawing).

ing pin. They are strongly correlated with an increase of the target temperature that was monitored by a thermocouple mounted directly on the Li metal. Usually, after the polarization had dropped by 10%, the target was replaced and the polarization then returned to its high value. The observed mean polarization of the target is in excellent agreement with calculations performed on the basis of the structure of the measurement cycle and the previously measured polarization transfer coefficient [53]. This confirms that the absolute polarization of the ^{8}Li nuclei is known with sufficient precision.

The time dependence of the asymmetry measured by the target polarization monitors during the data accumulation phase of the cycle is shown in Fig. 5. We observe an exponential decay of the asymmetry in time with a mean relaxation time of the polarization $T_1 \sim 3.5$ s, which is substantially longer than the 0.84 s half life of the decay. The extracted spin relaxation time T_1 is in good agreement with the values expected from the solid state models and from $^7\mathrm{Li}(\vec{n},\gamma)\,^8\vec{\mathrm{Li}}$ measurements [56].

As a byproduct, caused by variations of the temperature T of the target which have occurred due to inefficient cooling in our first run, we obtained a dependence of the relaxation time $T_1 = K/T$ with the Korringa constant $K = 300 \pm 10$ K s (Fig. 6).

3. Purity of the ^{8}Li source

In the early stages of the experiment, the β spectrum was checked for contamination by decays other than ^{8}Li. We use enriched ^{7}Li targets with 99.9% purity guaranteed by the supplier.[3] A spectrographic analysis showed that contaminants (primarily C, N, Cl, and heavy metals) were present at less than 300 ppm. The only contaminant reactions of concern are $^7\mathrm{Li}(d,{}^3\mathrm{He})\,^6\mathrm{He}$ and $^{16}\mathrm{O}(d,n)\,^{17}\mathrm{F}$, with Q values of -4.5 MeV and -1.6 MeV, respectively. The first reaction is inherently associated with the target material, while the second may occur in the oxide layer on the surface of the lithium metal. Such a stratum cannot be entirely avoided, despite such precautions as using an argon or helium atmosphere during the mounting of new targets. The potential contribution of the oxide layer is reduced because its thickness is a few orders of magnitude less than the ~ 1 mm range of the 10 MeV deuterons in lithium. The end point energies of the electrons emitted from ^{6}He and positrons from ^{17}F

[3]Oak Ridge National Laboratory.

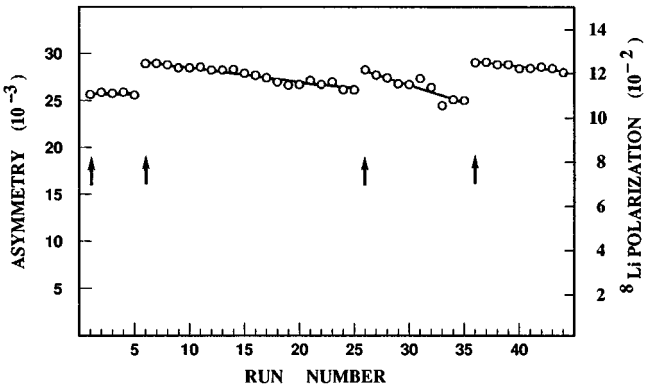

FIG. 4. Mean polarization of the ^{8}Li source observed during counting intervals over a five day measuring period. The lines are to guide the eye. The arrows indicate replacements of the ^{7}Li target.

decay are 3.5 MeV and 1.7 MeV, respectively. Since a 4 MeV energy threshold is applied for electrons accepted in the analysis of the data for the R coefficient, we do not expect any contribution from these sources in the final data sample.

Contributions of other β emitters activated in the vicinity of the target (e.g., in the collimators, target housing, etc.) were checked by measuring the energy spectrum of the electrons emitted from the source, and by the analysis of the time spectra from the monitor detectors in all of our on line measurements (Fig. 2, Ref. [48]). In a supplementary measurement with increased dwell time we did not detect traces of a long term activity that could build up by the irradiation of the apparatus or collimators (Fig. 7). We conclude that the contamination by electrons which do not originate from the ^{8}Li decay was less than 1%. This is sufficient to neglect contributions of contaminant activities in the data analysis.

C. Electron polarimeter

1. General idea

As briefly discussed in Sec. III A, the most suitable process to analyze the transverse polarization of electrons from

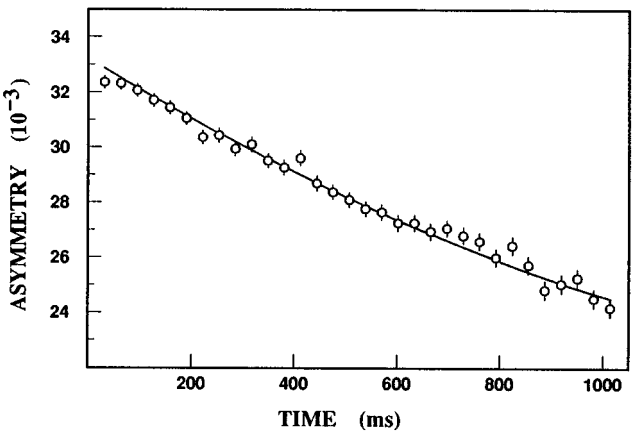

FIG. 5. Time dependence of the asymmetry measured by the monitor detectors. The solid line shows an exponential fit to the data with a spin relaxation time $T_1 = 3.5$ s.

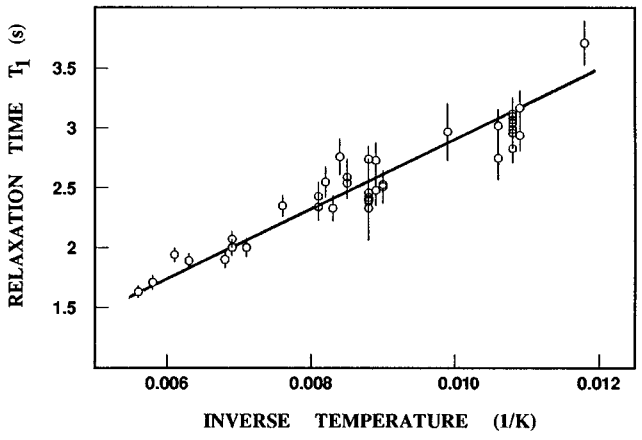

FIG. 6. Dependence of the spin relaxation time T_1 observed in this experiment on the inverse temperature $1/T$. The line is a fit to the data with the Korringa constant $K=300$ K s.

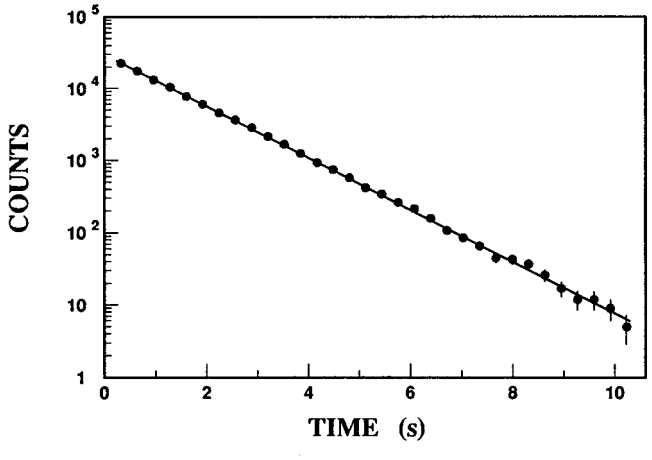

FIG. 7. Time spectrum from the monitor detectors. This measurement was performed immediately after few days of data taking with the highest beam current ($\sim 1.5\mu$A). Note the excellent agreement of the data with the exponential decay law with a *single* component corresponding to ^{8}Li decay. The fitted value of the lifetime, 836 ± 1 ms, is in agreement with the literature value 838 ± 6 ms [51].

β decay is Mott scattering. The calculated analyzing power[4] for scattering of electrons from lead nuclei in the energy and angular range of interest for this experiment is shown in Fig. 8. Appreciable values, ~ -0.1 to -0.5, are observed at large scattering angles, in the domain of low cross sections.

From the point of view of counting statistics as well as systematic errors, the most favorable conditions for a measurement of the R correlation are obtained for a configuration of mutually orthogonal directions of the nuclear polarization $\vec{J}$, the electron momentum $\vec{p}$, and the transverse polarization of the electron $\vec{\sigma}$. These requirements led to the idea of a high efficiency polarimeter.

The development of our design is shown in Fig. 9. The left side shows the simplest arrangement, consisting of the two up/down detectors and a scattering foil, to determine the transverse, time reversal violating component of the polarization for electrons emitted from the sample of polarized nuclei. The signal is proportional to the up/down asymmetry in the scattering. Axial symmetry implies that there is no azimuthal dependence in the emission of the electrons with respect to the spin axis of the nuclei. Therefore the simple configuration may be used repeatedly (Fig. 9, center). In a further step we are led to the idea of *only two* detectors in the form of *rings* (Fig. 9, right). Two such continuous ring detectors are capable of detecting the T-violating transverse polarization component by measuring the up/down asymmetry in the large angle scattering of electrons impinging on the continuous analyzer foil stretched around the median plane of the apparatus.

A polarimeter with axial symmetry has important advantages. Its large acceptance angles, both for electrons emitted from the source and those scattered toward the ring detectors, assure the required high efficiency. The symmetry of the apparatus is helpful in suppressing possible systematic effects arising, e.g., due to misalignment of the spin axis.

In the implementation for our experiment, each ring detector is subdivided into two 90° segments downstream of the target and two 60° segments upstream of the target, respectively (Fig. 10). Each segment consists of triple scintillation telescopes (δ,Δ,E). Such a structure of the polarimeter was convenient for practical reasons. First, small azimuthal dead layers are necessary to provide room for the beam pipe assembly, liquid nitrogen cooling lines for the target, and a slit for electrons emitted from the source toward the auxiliary counters $M_{u,d}$ (Fig. 10) that monitor continuously the polarization of the ^{8}Li target. In addition, division of the rings into four quadrants assures the possibility of a comparison of the results obtained from the various segments. This is an important cross check of the data. Using unsegmented rings would be hazardous, since the same con-

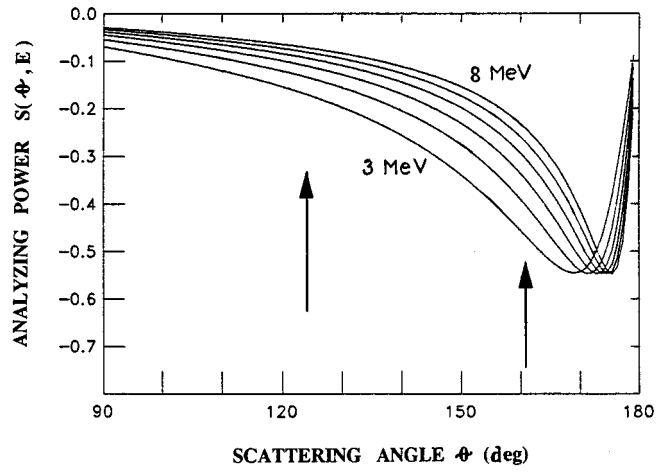

FIG. 8. Angular dependence and energy dependence (between 3 MeV and 8 MeV, 1 MeV step) of the analyzing power for electron scattering from lead nuclei. The arrows show the acceptance limits of our apparatus.

[4]Very recently, we completed a test of Mott theory in a scattering experiment with polarized electrons at Mainz Microtron. Very good agreement with the theoretical analyzing powers was found. See also Sec. IV B.

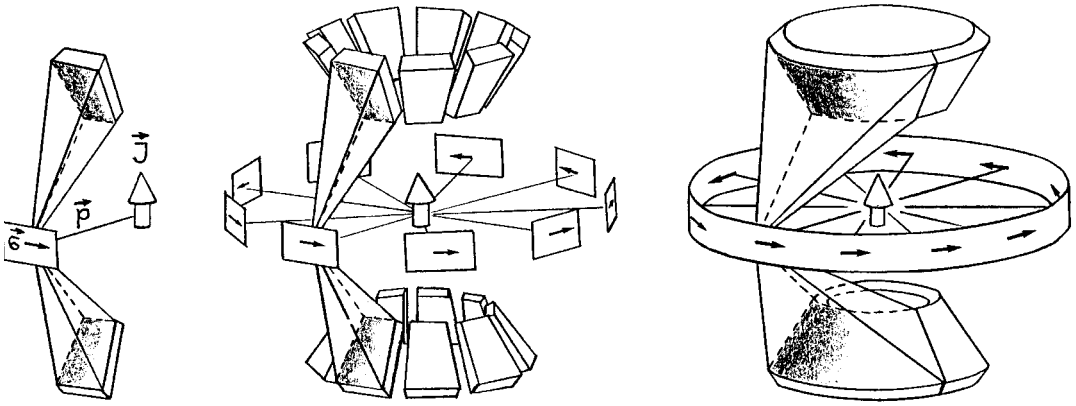

FIG. 9. The idea of an electron polarimeter for a measurement of the R correlation in β decay. The source of polarized nuclei is indicated by the large arrow $\vec{J}$. Left part: side view of the standard measurement of the transverse polarization $\vec{\sigma}$ (little arrows) of the electrons with the momentum $\vec{p}$, by a pair of up/down detectors. Middle: azimuthal independence of the decay process allows for using repeated arrangements of pairs of detectors and analyzer foils. Right: Multiple detectors are combined in an efficient and symmetric polarimeter in the form of two unsegmented rings. The shadowed areas correspond to solid angles covered by the detectors for scattering from a given point on the analyzer foil.

ditions for the detection of electrons are not guaranteed *a priori* for all azimuthal angles. For example, background radiation could be different for the upstream and the downstream part of the apparatus. We have found therefore that a moderate segmentation of the ring detectors provides important advantages in this experiment.

2. Design of the polarimeter

Figure 11 shows technical details of the polarimeter. Note the major alterations of the apparatus since our first publication (Ref. [48], Fig. 1). Our detection system is based on plastic scintillators. They assure a uniform and fast response which is important in discrimination against background, as well as being robust in the high radiation environment during target activation. We used 2 mm thick transmission and 4 cm thick stopping counters. The whole system consists of 28 scintillator modules utilizing 52 photomultiplier tubes.

In the development of the apparatus the reduction of background due to electrons, and their associated bremsstrahlung, which were not scattered from the analyzer foil was of paramount importance. In the early stage of the experiment we performed numerous tests with various materials and shapes to shield the detectors from the very intense radiation emitted from the ^{8}Li source. Our tests have shown that the best commonly available material for this purpose is brass. Substances with lower Z, e.g., plastics, turned out to be ineffective because of their low density, and aluminium exhibited an extensive β activity after capturing neutrons from the breakup of deuterons stopped in the Li target. The collimators in the central part of the shielding are shaped in such a way that at least two scatterings are necessary to reach the analyzer for electrons that are emitted out of the geometric acceptance angle of the foil. The ''shadow angle'' of the collimators exceeds the acceptance angle of the analyzer foil by almost a factor of 3. Lead was used for shielding only in the proximity of the scintillators and was never exposed to the electron radiation to avoid backscattering.

3. Tests of the detectors

The response of our detectors was investigated in offline tests with light emitting diodes (LED) and radioactive sources (^{90}Sr, ^{106}Ru), that were also used in calibrations. The variations of the response across the face of the detectors are shown in Fig. 12. We observe quite a uniform pulse height response to monoenergetic radiation for the stopping E de-

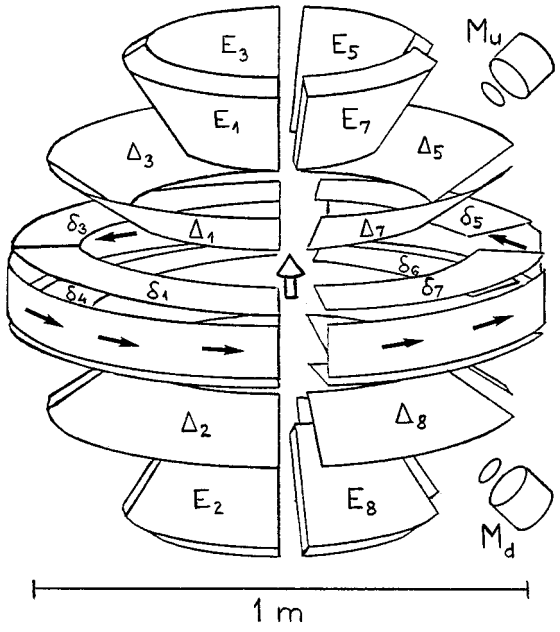

FIG. 10. Electron polarimeter used in the ^{8}Li R-correlation experiment. The electrons emitted at 90° with respect to the nuclear spin axis (large arrow in the center) impinge on the scattering foil with a large acceptance angle. The ring detectors are segmented into quadrants to provide independent measurements of the R correlation. The counters (M), mounted at 45° and 135° polar angles monitor the target polarization by detecting the regular β decay asymmetry. The deuteron beam comes from the right.

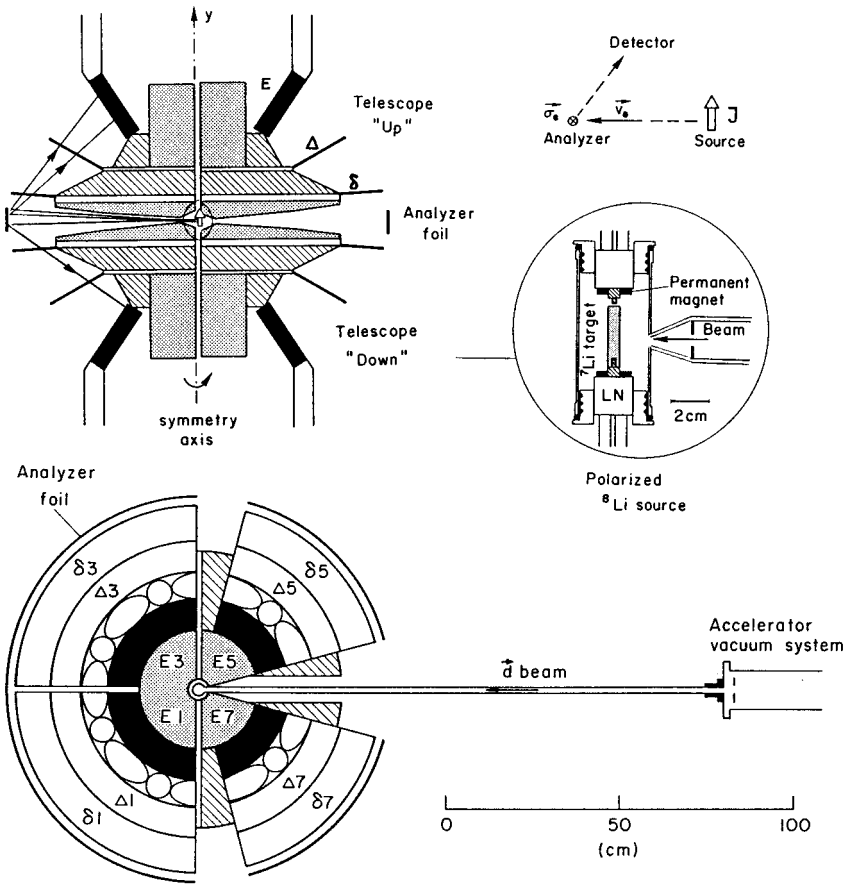

FIG. 11. Details of the setup. Upper part: vertical cross section; lower part: top view. A sample of polarized ^{8}Li nuclei is produced in the center of the apparatus by the polarized deuteron beam that enters from the right. The detectors are surrounded by passive shields (hatched areas) protecting them from the intense primary radiation emitted from the ^{8}Li source. The inset shows details of the target chamber. The last section of the beam pipe ($\sim$ 1.5 m) and the housing of the target are made of lucite to minimize backscattering of electrons from objects other than the lead analyzer foil. Electrons emerge from the target chamber through a thin, 70 μm Kapton window.

tectors. A stronger dependence for the transmission counters does not pose a problem since their pulse height does not enter the analysis of the experiment. These thin detectors deliver a low light output, therefore we have proven that the electron pulses were well separated from the noise. A typical pulse height resulting from the light produced by $\sim$2 MeV electrons (minimum ionization) in the transmission counters was $\sim$100 mV compared to the largest dark current noise of 20 mV.

The energy resolution of the stopping detectors was scanned with light emitting diodes (LED) that were embedded into scintillators in the most distant place from the photomultipliers. Pulse height spectra of the LED's are shown in Fig. 13.

The extracted resolution varies with the energy according to $0.3/\sqrt{E(\mathrm{MeV})}$, as expected from photon counting statistics. Taking into account the position dependence of the response we obtain an energy resolution of $17\pm2\%$ at 4 MeV, which corresponds to the threshold that was used in the analysis of the data. The resolution has been verified at low energies in measurements of spectra from β sources, and at higher energies ($\sim$10 MeV) by observing hard cosmic radiation.

4. Energy spectra in the experiment

The use of triple telescopes directed toward the analyzer foil was essential in reducing the sensitivity to background radiation. With the arrangement shown in Fig. 10 and Fig. 11 we have observed a signal (scattering foil in place) to background (foil removed) ratio above the 4 MeV threshold of

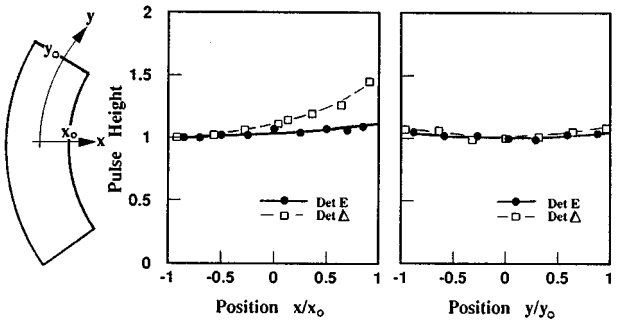

FIG. 12. Position dependence of the pulse height of the detectors. The inset on the left defines the coordinates. We checked that the pulse height variation for the δ counters was less than for the Δ detectors.

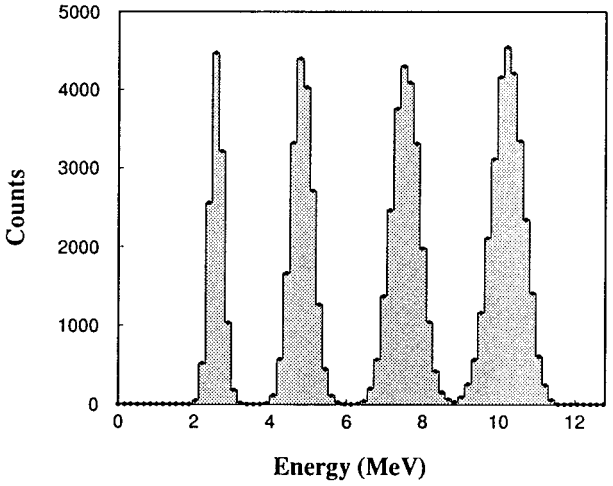

FIG. 13. Energy resolution of the stopping detectors measured with light emitting diodes. The energy calibration for electrons is shown on the horizontal axis.

14:1. Figure 14 shows the energy spectra of the stopping counters E in coincidence with Δ, δ detectors, taken in various conditions.

5. Electronics and data acquisition

A similar time response of all detectors allowed the use of a compact electronic setup. All signals from the photomultipliers (PM) were calibrated and synchronized in time with the aid of radioactive sources and light emitting diodes (LED). The pulses from the PM's viewing the same scintillator were added, and the electronics processed only one signal from each detector. First of all, fast coincidences were formed, providing a gate for the linear signals fed into fast, charge sensitive ADC's. A common gate was used for all ADC's, to equalize dead time losses for all the detectors. A number of scalers recorded the rates of the discriminators. A separate branch of fast electronics processed signals from the detectors monitoring the polarization of the ^{8}Li source. Pulses from the semiconductor Si detectors, measuring protons from the $^{12}C(d,p)^{13}C$ reaction that was used to monitor the polarization of the deuteron beam, were amplified and analyzed by slow, peak sensing ADC's.

The measurements were controlled by a processor[5] resident in the CAMAC crate. Its task was to define and coordinate the time structure of the measurement, e.g., to provide control signals for the beam chopper, radio frequency transitions at the ion source, and for LED's that have monitored continuously the gains of all E detectors. The main data flow was controlled by a CAMAC based front end processor[6] and directed via ETHERNET to the μVAX back end computer. The data were recorded as a function of time T after activation of the target (32 time bins, 33 ms duration each) and energy deposited in the detectors (64 energy bins). The following energy$\times$time ($E\times T$) spectra of the ring polarimeter detectors were recorded on the disc for the two polarization

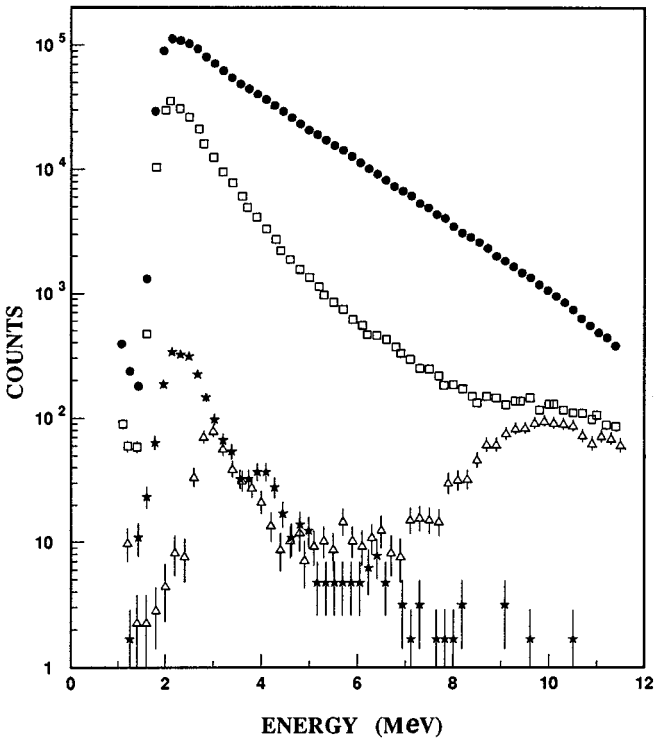

FIG. 14. Energy spectra acquired in $\sim$ 2 hours. Filled circles: regular measurement of electrons emitted in the decay of ^{8}Li and scattered from the 35 mg/cm^2 lead foil surrounding the apparatus. Squares: background measurement with the foil removed and the Li target activated by the deuteron beam pulsing according to the regular measurement cycle (Fig. 3). Triangles: "no beam" measurement—room and cosmic background. Stars: accidental coincidences acquired in the same conditions as for regular measurements.

states of the ^{8}Li source: $\Delta E\times T$, $E\times T$, $(E+\Delta E)\times T$, $E_{\rm LED}\times T$. Additionally, spectra from the polarization monitor detectors (M) were recorded, as well as a high rate pulser fed into scalers for dead time control, and the information concerning beam current on the target. Altogether 92 spectra, most of them two-dimensional, were stored on the disc for the off-line analysis.

IV. SIMULATION OF THE EXPERIMENT

Extensive computer simulations were used in the early stages of the experiment to define optimal geometrical conditions for the layout of the detectors. Later, the results of these calculations were compared to the data, to assure our understanding of the response of the apparatus.

A. Effective analyzing power

The effective analyzing power of the polarimeter was one of the important results of the simulations. It was pointed out repeatedly [57] that the theoretical values of the Mott analyzing powers may be used with confidence for electrons with energies in the range of a few MeV. These energies are high enough to make screening of the nucleus by atomic electrons ineffective, and they are sufficiently low to cause only tiny effects due to finite nuclear size.

[5]"Firecracker" ACC 2160, Creative Electronics Systems.

[6]"Starburst" ACC 2180, Creative Electronics Systems.

Two independent simulations, based on different approaches have been developed by subgroups of our collaboration at the ETH Zürich and at the University of Wisconsin. In one simulation numerical integration was used, while the other was based on a Monte Carlo technique.

The most important calculated quantities were the effective cross section $\langle\sigma\rangle$ and the analyzing power $\langle S\rangle$ of the polarimeter:[7]

$$\langle\sigma\rangle=\frac{1}{H}\int_T^{E_{\max}}P(E)\int_{-H/2}^{H/2}\int_\Omega\left(\frac{d\sigma}{d\Omega}\right)_M(E,\theta)d\Omega\,dh\,dE,$$

$$\langle S\rangle=\frac{1}{\langle\sigma\rangle H}\int_T^{E_{\max}}P(E)\times\int_{-H/2}^{H/2}\int_\Omega\left(\frac{d\sigma}{d\Omega}\right)_M(E,\theta)S_M(E,\theta)\cos\phi\,d\Omega\,dh\,dE.$$

Here T denotes the low energy threshold for electrons accepted in the data analysis, $P(E)$ is the ^{8}Li β decay spectrum with its integral over the energy E normalized to unity, and H is the height of the scattering foil. The scattering angle with respect to the axis defined by the momentum of the electron impinging on the foil is θ, and ϕ is the angle between the component of the transverse polarization (in the median plane) and the normal to the scattering plane of the electrons. The Mott cross section and analyzing power are denoted by $d\sigma/d\Omega)_M(E,\theta)$ and $S_M(E,\theta)$, respectively, and the integrals $d\Omega,dh$ run over the ''geometry'' of the apparatus. The acceptance angles θ of our polarimeter are $124°<\theta<161°$.

We note that no great accuracy in the calculations of the effective analyzing power of the apparatus is required for this experiment. The uncertainty in the calibration of the polarimeter comes as a multiplicative factor into our final result, as well as into the error, and therefore it does not influence our conclusions concerning presence or absence of the T violation effect. Obviously, in order to use our result as a limit for couplings of exotic interactions or masses of the exchanged particles, we must ensure that the final error of the experiment is estimated with appropriate precision. However here, according to general rules [2], a 10% accuracy in the analyzing power of the polarimeter is adequate.[8]

The procedure for the calculation of the Mott scattering from the Dirac equation, though tedious, is well established [57]. The formalism belongs to the classics of scattering theory. Details of our calculations may be found in Ref. [58], which also contains the very first results of this experiment. There is no doubt that the values of the Mott analyzing power can be calculated with a precision of a few %. This was tested by comparing the results obtained with our two independent programs to the abundant analytical data [57]. The agreement is on the level of 3%. We compared also the results of our calculations to the absolute values of the analyzing powers *measured* in double scattering experiments. The highest reported energies for such measurements are 0.204 MeV and 0.261 MeV. Once again an agreement $\sim$3% has been found between the calculated and measured analyzing powers at 105°. Additionally, cross sections generated by the program were compared to the measured values [59] exhibiting slightly less good agreement ($\sim$ 15%), which could be attributed mostly to normalization errors. The analyzing power of the apparatus, averaged over the energy of the scattered electrons and not including depolarization effects, is -0.125.

B. Depolarization effects

Since the dominant contribution to the error of the experiment comes from the counting statistics, an increase in the foil thickness could bring an appreciable gain in the accuracy. However, depolarization effects prevent us from using thick analyzer foils. Therefore, we asked the following question: what thickness of the foil guarantees the required 10% accuracy in the effective analyzing power?

Estimations of the proper foil thickness were done independently with the two simulations discussed above. In one of the programs we applied the analytic procedure for the depolarization [60] that has been tested in the experiments; the other approach was once again a Monte Carlo (MC) simulation. We verified the accuracy of the multiple scattering correction by MC calculations for the precise measurements of the asymmetry in the scattering of polarized electrons from Au foils. At 0.616 MeV and a 2.21 mg/cm^2 thick foil, that provides a multiple scattering angular distribution similar to our experiment, Brosi *et al.* [61] measured an asymmetry of 0.195 ± 0.003. The MC simulation gives 0.186. For nine measurements with Au foil thicknesses between 0.44 and 6.27 mg/cm^2, corresponding to measured asymmetries between 0.304 and 0.093, we obtain very good agreement: the ratio of the MC generated to the measured asymmetries amounts to 1.02 ± 0.05. These tests of the calculations were reported elsewhere [48]. In later data taking periods we performed a further test by comparing our measurements to the generated electron spectrum altered by the multiple scattering processes. The effects of multiple and plural scattering were increased by using 175 mg/cm^2 foils, much thicker than the 35 mg/cm^2 used in the measurements of the R correlation. The simulated spectra account for 95%

[7]Angular and energy dependent Mott analyzing power is widely known as ''Sherman function,'' particularly in atomic physics applications. Therefore we use the abbreviation S for the Mott analyzing power, to avoid conflicts with the β decay asymmetry parameter A.

[8]An elegant method to obtain the effective analyzing power of our system would use the transverse component of the electron polarization arising due to the time reversal conserving N correlation [50]. In such a calibration experiment one could use the same apparatus as in regular measurements of the R coefficient and, in principle, no reliance on the results of the simulation would be necessary. This experiment would take care of averaging over the finite size of the detectors, the depolarization effects in the analyzer foil, etc. However, this method is impractical. The expected value of the N correlation parameter for the ^{8}Li decay is only $\sim3\times10^{-2}$. It would require much more beam time than used in all our measurements performed up to now to calibrate the polarimeter with a 10% statistical accuracy by using the N correlation.

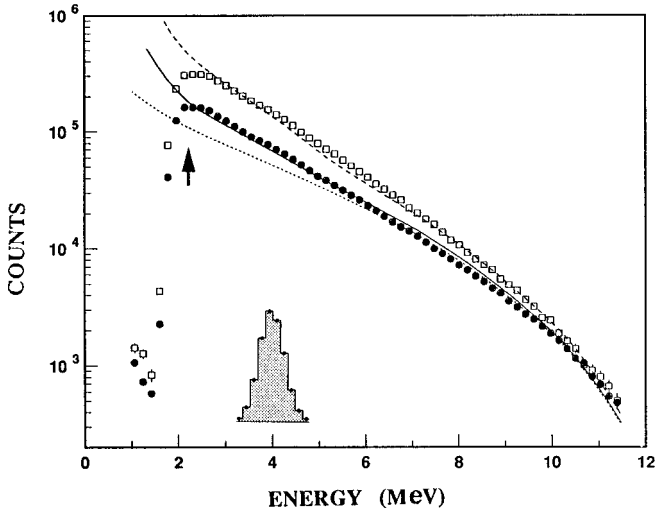

FIG. 15. Energy spectrum of electrons scattered from the 35 mg/cm^2 (filled circles) and 175 mg/cm^2 (open squares) lead foils. All background events were subtracted. The arrow shows the position of the hardware discriminators. The Monte Carlo predictions are shown as solid and dashed lines, respectively. The dotted line shows a calculation without multiple scattering corrections. The inset shows the energy resolution of the detectors.

of the measured events with an electron energy above 4 MeV, and the energy dependence of the correction is well reproduced by the calculations, even for the very thick foils (Fig. 15).

Recently, we have performed a measurement of the analyzing power and depolarization effects in thick scattering targets using a polarized electron beam from the Mainz Microtron (MAMI). The results obtained at 14 MeV [62] were scaled to lower energies, showing once again very good agreement with our earlier estimations. The experiment at MAMI is a separate project, still in progress; the final results will be published elsewhere after its completion. We conclude that the multiple scattering corrections are known to the required precision.

The energy dependence of the analyzing power for our polarimeter with and without multiple scattering (MS) corrections is shown in Fig. 16. Very good agreement of the results for the two calculations was obtained in the region of interest, above 4 MeV. At low energies the uncertainties associated with multiple scattering grow rapidly, and in fact both calculations become unreliable for electron energies below 1.5 MeV.

In conclusion, the average analyzing power of the polarimeter for electrons with energies higher than 4 MeV is -0.100, if multiple scattering effects are included. After experimental tests of our calculations, in particular these at the accelerator with a polarized electron beam, we consider it justified to lower the systematic uncertainty associated with the depolarization of the electrons in the analyzer foil from 10% quoted in Ref. [48] to 7–8 %.

Estimations based on the theory which describes depolarization of the electrons following β decay in thin radioactive sources [63] show that the effects of small angle multiple scattering in the ϕ 5 mm Li target are less than 0.2%. Large angle plural scattering, that has contributed to the depolarization in the Pb foils, is entirely negligible in this case due to the much lower charge of Li. Similarly, the depolarization in the Kapton windows and in the air between the ^{8}Li source and the scatterer is also negligible.

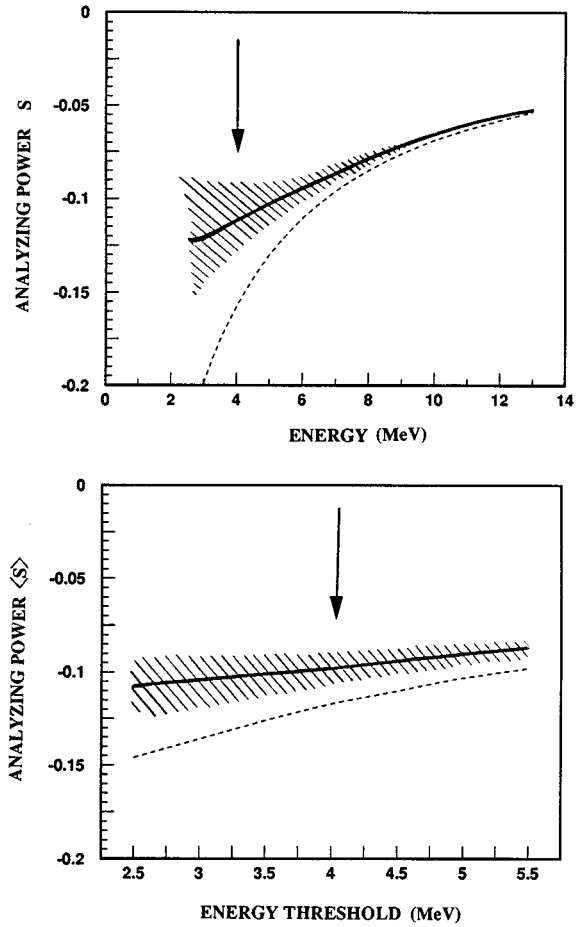

FIG. 16. Upper part: energy dependence of the analyzing power of our polarimeter; lower part: effective analyzing power (energy averaged) as a function of the energy threshold for electrons accepted in the analysis. Dashed lines: without multiple scattering corrections; solid lines: multiple scattering corrections included. Estimated uncertainties are shown as shaded areas. The arrows indicate energy threshold actually used in the analysis.

C. Systematic effects

Since the effective analyzing power of the polarimeter amounts to -0.10 and the polarization of the ^{8}Li source is ~ 0.12, a statistical error of $\sim 10^{-5}$ in the asymmetry is needed to achieve an error in the R coefficient $\sim 10^{-3}$. Therefore, systematic effects must be mastered at the level of few times 10^{-6} in the measured asymmetry.

A number of systematic effects were considered. Besides depolarization, which was already discussed, they include nonuniform illumination of the scattering foil, misalignment of the spin direction, gain shifts of the photomultipliers, background radiation, accidental coincidences, etc. Corrections or limits for disturbing effects were obtained in additional measurements. All corrections with uncertainties determined by counting statistics in the auxiliary measurements will be discussed in Sec. V, where numerical values of all

contributions will also be presented.

By far the most interesting effect of a nonstatistical nature is associated with the nonuniform illumination of the scattering foil. The effect arises from a combination of the parity violating β decay asymmetry and geometric extensions of the apparatus, in particular the scattering foil. Figure 17 shows the abbreviations used in the discussion below.

The intensity distribution N for electrons impinging at the height h on the scattering foil above (positive h) or below (negative h) the median plane is given by

$$N\left(\alpha=\frac{h}{r}\right)\sim 1+JA\cos\theta\approx 1+JA\alpha,$$

where θ is the polar angle with respect to the nuclear spin axis, α is the corresponding angle measured from the median plane ($\alpha=\pi/2-\theta$), r is the radius of the foil, J is the polarization of the target, and A the decay asymmetry parameter. Electrons impinging on the scattering foil above the median plane are obviously closer to the upper (u) than to the lower (d) ring detectors. Therefore, even in the case of a perfect alignment of the detectors, the two u,d telescopes have different acceptances if $h\neq 0$. Expanding the product of the effective cross section and solid angle $\sigma\Omega$ to second order in the small parameter $\alpha=h/r$, we obtain

$$(\sigma\Omega)_d^u=(\sigma_0\Omega_0)\left[1\pm\alpha\frac{1}{(\sigma_0\Omega_0)}\frac{\partial}{\partial\alpha}(\sigma\Omega)\big|_0+\alpha^2\frac{1}{2(\sigma_0\Omega_0)}\frac{\partial^2}{\partial\alpha^2}(\sigma\Omega)\big|_0+O(\alpha^3)\right],$$

where the derivatives are taken at $\alpha=0$. The rate measured in each detector is proportional to the integral of the product $N(\sigma\Omega)$ over the height of the scattering foil. Forming the asymmetry ε we obtain

$$\varepsilon=\frac{[\int N(\sigma\Omega)_u-\int N(\sigma\Omega)_d]d\alpha}{[\int N(\sigma\Omega)_u+\int N(\sigma\Omega)_d]d\alpha}=\frac{1}{3}\alpha_0^2(JA)\rho+O(\alpha_0^4),$$

where α_0 is the limiting angle of the foil, and ρ is the slope parameter. Since in our experiment $\alpha_0\approx 0.05$ radians, higher order terms contribute at the 10^{-3} level of the leading term, and may be safely neglected (the correction from the leading term is in the order of the final error bar of the experiment).

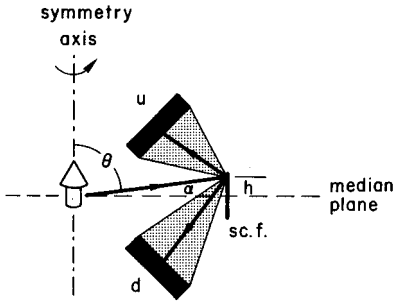

FIG. 17. Definition of symbols used in the derivation of the correction due to nonuniform illumination of the scattering foil. The figure shows a vertical cut through the experimental arrangement.

The product JA was continuously measured with the two polarization monitors M mounted at $\theta\approx 45°$. The parameter ρ,

$$\rho=\frac{1}{(\alpha_0\Omega_0)}\frac{\partial}{\partial\alpha}(\sigma\Omega)\big|_0,$$

was determined in auxiliary measurements using a narrow (1 cm) scattering foil. The foil was displaced from the median plane, and the rate was measured as a function of the angle α. This rate, normalized to the rate observed with the foil in the median plane, provides the slope parameter ρ (Fig. 18). We measured $\rho=2.8\pm 0.4$, while our simulations predicted $\rho=2.6\pm 0.1$.

Since the intensity N changes in step with the reversal of the target polarization, the false asymmetry caused by this spurious effect also changes its sign, and therefore simulates a nonzero time reversal coefficient R. The only means to diminish the undesired effect due to β decay asymmetry is to reduce the acceptance angle α_0 by using a narrower analyzer foil (Fig. 18). However, this can be done only at the expense of the rate of ''good'' events, since we do not wish to increase simultaneously the thickness of the foil due to the growing importance of the depolarization factor.

In contrast to the β decay asymmetry, geometrical imperfections in the positioning or shapes of the detectors and scattering foil stay the same when the target polarization is reversed, and therefore their effects cancel when the spin averaging of the measured asymmetry is performed (e.g., by the well known ''double ratio'' method). For example, easy to achieve accuracy of few mm in the positioning of the scattering foil is satisfactory at the present accuracy of the experiment.

The finite extension of the ^{8}Li source (1.5 mm$\times$2 mm $\times$6 mm) is negligible in this experiment. Other geometric effects, e.g., due to misalignment of the symmetry axis of the apparatus and the spin axis of ^{8}Li nuclei are strongly suppressed. Consider for example a typical misalignment angle of $\zeta\sim 1°$. This may produce transverse components of the polarization in the median plane of the polarimeter via the time reversal conserving N correlation [50]. These components will reverse in step with the polarization of the source and, in principle, they may lead to a spurious effect. However, a transverse polarization p_N due to N correlation is small for relativistic electrons. For ^{8}Li decay, at energies greater than 4 MeV, $p_N\sim 3\times 10^{-2}$ [50]. Only the projection of this polarization ($\sim p_N\sin\zeta$) onto the plane of the scattering foil may produce a systematic effect. The largest modulation of this projection appears for two regions on the foil that lie in the direction perpendicular to the plane defined by the two misaligned axes. Finally, the anticipated false asymmetry has opposite signs for the two considered regions on the foil. Therefore, for an axially symmetric apparatus the resulting effect is zero. Detailed calculations show that the suppression factor due to the symmetry of our polarimeter is about 0.1. Therefore, we can set a limit of $\sim 5\times 10^{-5}$ for the false contribution to the R correlation from the misalignment of the axes. This limit is lower by two orders of magnitude than the present accuracy of the experiment, and therefore such effects are entirely negligible.

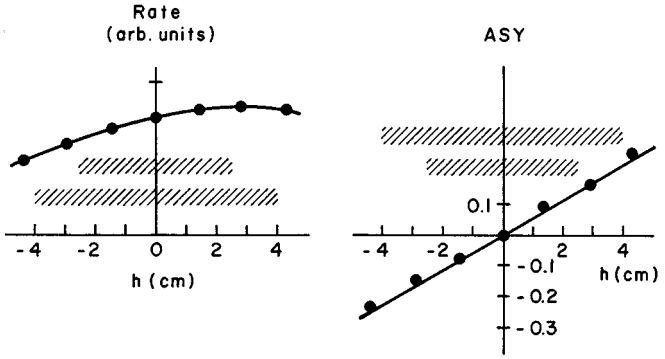

FIG. 18. Left side: rate measured by the polarimeter detectors as a function of the position of the auxiliary, 1 cm narrow scattering foil. Right side: asymmetry in the rate, which provides the slope parameter ρ discussed in the text. In the course of the experiment we reduced the height of the main analyzer foil (shaded range) in order to reduce the disturbing effect.

V. DATA ANALYSIS

A. General concept

Neglecting instrumental effects, the expected rates w_d^u in the up (u) and down (d) detectors, placed at the same angles and measuring scattered electrons with the polarization $\vec{\sigma}$, are

$$w_d^u = w_0[1 + S(\vec{\sigma}\vec{n}_d^u)].$$

Here S is the analyzing power of the scattering process and $\vec{n}_d^u = (\vec{v}\times\vec{v}_d^u)/|\vec{v}\times\vec{v}_d^u|$ are the unit vectors perpendicular to the scattering plane that is defined by the velocities of the incident and scattered electrons $\vec{v}$, $\vec{v}_d^u$, respectively.

The transverse, time reversal violating component of the polarization $\vec{\sigma}_T$ is proportional to the polarization of the decaying nucleus $\vec{J}$:

$$\vec{\sigma}_T = R\left(\vec{J}\times\frac{\vec{v}}{c}\right).$$

This relation defines the correlation coefficient R which is the goal of our measurement. The (v/c) velocity dependence of $\vec{\sigma}_T$, expected from theory (Sec. III), is explicitly singled out. In our case, for electrons with energies greater than 4 MeV, $1 > v/c > 0.994$, and the velocity factor can be neglected. Since $\vec{\sigma}_T$ changes sign with the reversal of the nuclear polarization, we combine the last two formulas for electrons emitted at right angles to the nuclear spin axis to obtain

$$w_d^u = w_0[1 \mp SRJ],$$

where J is a positive (negative) number when the nuclear polarization vector points up (down). Defining the "double ratio"

$$r_R = \sqrt{\frac{w_+^u w_d^-}{w_-^u w_d^+}}$$

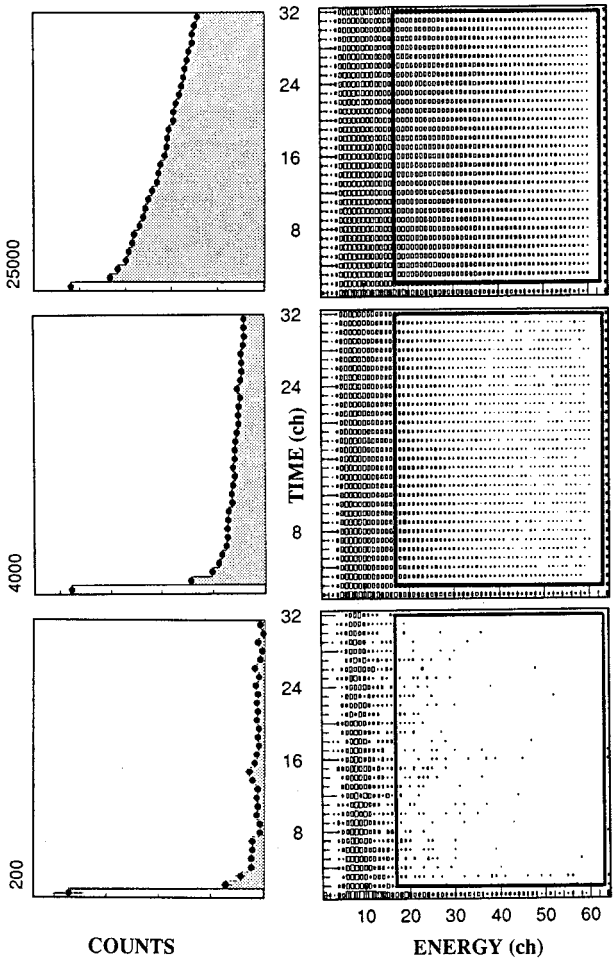

FIG. 19. Raw data. Right side: electron energy vs decay time (0.2 MeV $\times$ 33 ms bins). Upper part: scattering foil in place; middle part: foil removed; lower part: accidental coincidences with the foil in place. Left side: projections on the time axis. Note a significant excess of events in the first time channel and different scales in the three panels. Corresponding projections on the energy axis are shown in Fig. 14.

for the two detectors u, d and the two polarization states $+,-$ of the target, we obtain the asymmetry[9]

$$\varepsilon_R = \frac{r_R - 1}{r_R + 1} = -SR|J|.$$

The nuclear polarization J is obtained from the analysis of the data provided by the monitor (M) detectors. The analogous relation for monitors is

$$\varepsilon_M = \frac{r_M - 1}{r_M + 1} = A|J|\cos\theta,$$

where θ is the polar angle of the monitor detectors and A is the β decay asymmetry parameter.

[9]The advantages of this procedure are well known and were repeatedly discussed, therefore here we only recall that detector efficiencies, solid angles, and activity normalization cancel in the ratio r_R.

TABLE II. Important experimental parameters for various data collection periods.

Run period	I	II	III	IV
Apparatus	Quarter	Half	Complete	Complete
Angular coverage	25%	50%	85%	85%
Detectors	Δ,E	δ,Δ,E	δ,Δ,E	δ,Δ,E
Deuteron beam (nA)	250	400	300	300−1500
^{8}Li polarization	0.10	0.11	0.12	0.11
Scattering foil (mg/cm^2)	27	35	35	35
Scattering foil height (cm)	8	7	6	5
Analysis threshold (MeV)	3	4	4	4
Signal/background	10	14	14	12

For extended detectors counting electrons in a broad angular and energy range, an effective analyzing power $\langle S \rangle$ must be used (Sec. IV) as well as the time average of the nuclear polarization over the counting interval.

The formulas discussed are exact only in the absence of the disturbing effects due to background radiation, accidental coincidences, etc. These effects do not exhibit the same dependence on the energy and time elapsed after the activation of the target as the rates of the electrons scattered from the analyzer foil. Our experiment provided detailed data on these dependences. This enables a number of statistical analyses, which are sensitive to various potential sources of errors in the experiment.

B. Data characteristics

Data for the analysis of the R correlation in the ^{8}Li decay were acquired in four data collection periods extending over three years. Table II shows the values of the most important parameters for these measurements.

Documentation of the development of the experiment may be found in conference proceedings [64]. The results of the first two data taking periods, obtained with incomplete apparatus, were published in Ref. [48]. We will focus here on the last two series of measurements that have provided the bulk of collected data ($\sim$90%).

C. Analysis procedures

Most of the data were accumulated in runs of 2 hour duration. One quarter of the collection time was devoted to measurements with the regular irradiation pattern, but with the scattering foil removed. These measurements provided data on the intensity and asymmetry of the background radiation that affected each of the telescopes. Figure 19 shows raw data for typical runs with the scattering foil in place, foil removed, and for a measurement of the accidental coincidences.

The general procedure was to calculate separately uncorrected R coefficients for foil-in measurements and R coefficients for disturbing effects, and to subtract fake contributions using weights defined by the measured intensities. This procedure was applied for five distinct classifications of the data into subsets, that resulted in a vastly different number of degrees of freedom in the statistical analyses. It was checked that the same results were obtained by applying corrections on the level of asymmetries instead of R values.

In the five analyses all the accumulated data were used. We applied the same criteria for the data selection as in our previous investigation [48]. Only electrons impinging on the scattering foil with energies higher than 4 MeV were considered, to avoid depolarization effects.[10] The first time channel (33 ms) after activation of the target was always disregarded. We have observed a significant excess of events in this short time interval, particularly for the foil-out data and accidental coincidences (Fig. 19). A part of this excess may contain events associated with the tail of the beam not yet completely deflected at the ion source and accelerated to the target,or with short living activities. In addition, in the very first time channels, the photomultipliers and their electronics have not yet reached a steady state, recovering from a flash of light produced in the scintillators by neutrons and γ rays that have penetrated the passive shields during the activation of the target. Due to the unfavorable background conditions, the statistical impact of the data collected in the first time channel is reduced to $\sim$ 1% of the final error, and therefore these data were not analyzed.

We describe here details of the different data analyses with a discussion of their advantages and shortcomings.

(1) Cumulative analysis. The simplest treatment of the data. All foil-in (signal) and foil-out (background) data for ring detectors, as well as for polarization monitors and beam integrators, were added into cumulative files. Counts were then integrated above the energy and time thresholds. An average value -0.100 of the analyzing power weighted by the energy spectrum of the scattered electrons (Fig. 16, lower part), and an average polarization of the ^{8}Li target, varying from run to run between $0.10-0.12$ (Table II), were used. R

[10]The analysis threshold of 3 MeV that was used for the first data collection run was raised to 4 MeV as a consequence of increasing the thickness of the foil from 27 mg/cm^2 to 35 mg/cm^2 (Table II).

coefficients were calculated for the four pairs of the corresponding up/down detectors. The background radiation was assumed to be constant for each detector during the whole data collection period. A distinction between detectors is made, since they operate under slightly different background conditions (particularly parts of the apparatus upstream or downstream of the target). Four statistically independent R-coefficient measurements (four pairs of detectors) yielding the final R value were obtained.

(2) Energy dependence. No detectable energy dependence of the R coefficient is expected from the theory, therefore our motivation was rather to check the consistency of the data, than to search for a real effect. The data were combined as in the analysis (1); however, 1 MeV broad energy slices were analyzed separately. The analyzing power was no longer constant, varying according to the upper part of Fig. 16. The final value of R is obtained by averaging 28 data points (4 pairs of detectors and 7 energy bins).

(3) Energy and time dependence. R coefficients were calculated on an energy$\times$time grid formed in the cumulated files. The detailed energy dependence of the analyzing power (Fig. 16) as well as the decrease of the target polarization due to spin relaxation phenomena (Fig. 5) were taken into account. In this analysis, we encountered the problem of calculating asymmetries from a small number of counts: for a fine grid ($\sim$200 keV $\times$33 ms), the content of channels corresponding to electrons with high energies ($\sim$ 10 MeV) that were emitted at the end of the measuring interval becomes very small (upper right corner of Fig. 19). Therefore, we rejected data corresponding to channels where at least one bin N_+^u, N_-^u, N_d^+, or N_d^- was zero.[11] For example, in the analysis of the third measuring period, we obtain in this way 5538 raw R coefficients. Since the positions of the channels with zero content for foil-in and foil-out data do not always match, the number of data points after applying corrections was reduced further to 5526 (apparent difference in N_{DF} entries in Table III). The large number of R coefficients obtained in this procedure allows for testing details of their distribution. An excess of the data with unexpectedly large deviations from the mean might suggest a systematic effect in the experiment.

(4) Slowly varying backgrounds. The assumption of a background stable over the whole data collection period was abandoned. In contrast to analysis (3), where all the data were added, here only 3 consecutive raw data files (6 hours) were cumulated and combined with the following background measurement. The time dependence of the background corrections could be studied, and once again runaway data points could be detected. The problem of small number of counts in certain channels is more acute here than in analysis (3) and it leads to the reduction of the 38383 data points to 37790 that are left after applying corrections.

[11]These details are discussed, since losses of data might be a main source of discrepancies between the results obtained from various analyses. The effects are bigger than intuitively expected: 1% differences in the data sample may lead to inconsistencies in the final results as large as $\sim$10% of the error bar. This is therefore the level of agreement to be expected between the results of different procedures.

In the analyses (1)–(4) we have restored the one-to-one correspondence between the signal and the background data by adding foil-in data into cumulative files. In this way correlations between the corrected results were avoided and statistically independent values for the corrected R coefficients were obtained in each case. Standard rules for calculations of the averages and the errors could then be used in the procedures described above.

(5) File by file analysis. Obviously a natural choice. We note that subtraction of a *common* background from few (usually 3) consecutive data files introduces *correlations* between the results. Although in this experiment such correlations are rather weak (low intensity of the background) and they therefore should not influence strongly the final result, some care must be exercised in a proper calculation of *the errors*. To avoid the problems discussed above with the rejection of some data, this analysis was performed with the energy$\times$time integrated spectra (108 correlated R measurements).

The procedures discussed here provide R-coefficient data that contribute to the final result, with vastly varying error bars ($\sim$0.01–1.0) and number of degrees of freedom. Applying tests of statistical consistency, we checked therefore in each case the χ^2/N_{DF} values as well as the corresponding confidence levels (Table III).

D. Corrections

1. Decay associated background

At first, the correction with the largest uncertainty ($\sim$1/2 of the final error bar) will be discussed.

The fraction of events that do not originate from electrons scattered by the analyzer foil is $\sim$0.07. This background radiation was inspected periodically by removing the scattering foil. As a rule one background measurement followed three runs with the foil in place.

For data analyses (1)–(4) we define

$$R = R^r + R^c,$$

where R is the result corrected for the disturbing effect, R^r is the raw value, R^c is the correction due to background radiation. We express the asymmetry corresponding to scattering from the analyzer foil by the measured foil-in and foil-out events:[12]

$$R = \frac{1}{J^r S}\frac{N_+ - N_-}{N_+ + N_-} = \frac{1}{J^r S}\frac{(N_+^r - N_+^b) - (N_-^r - N_-^b)}{(N_+^r - N_r^b) + (N_-^r - N_-^b)}$$
$$= \frac{R^r - (J^b/J^r) I R^b}{1 - I}.$$

Here, N denotes integrated counts for a given subgroup of data [e.g., each element of the fine grid in the analysis (3)], the indices $+$ and $-$ define the polarization state of the target, and the superscripts r, b refer to the "raw" (foil-in) and background (foil-out) data, respectively. The polarization of

[12]For simplicity, a single detector spin $+/-$ asymmetry is considered; the detector index is suppressed.

TABLE III. The results for series III of measurements, obtained with the five procedures discussed in the text. All R values and corresponding errors are in units of 10^{-4}. The results of statistical tests are attached.

Analysis	1	2	3	4	5
Raw data	-123 ± 71	-125 ± 69	-130 ± 70	-131 ± 70	-128 ± 70
N_{DF}	3	27	5537	38382	107
χ^2/N_{DF}	1.75	1.30	1.00	1.02	1.07
Confidence level	0.15	0.14	0.47	0.01	0.31
After decay background subtraction	-74 ± 82	-74 ± 82	-74 ± 83	-72 ± 83	-87 ± 81
N_{DF}	3	27	5525	37789	107
χ^2/N_{DF}	0.97	0.99	0.99	0.95	0.98
Confidence level	0.40	0.47	0.64	1.00	0.55

the target is denoted by J and the analyzing power of the polarimeter by S. The intensity ratio I is defined as

$$I=(N_+^b+N_-^b)/(N_+^r+N_-^r).$$

Using the formulas above we obtain the value of the background *correction*:

$$R^c=\frac{I}{1-I}\left(R^r-\frac{J^b}{J^r}R^b\right).$$

As expected, the corrections are small when the background intensity is low and when the raw and background R coefficients R^r, R^b have similar values.

In the derivation above we have assumed tacitly that the activity of the target is the same for the raw and background data. In the data evaluation, the counts N_+^r, N_+^b, ... were normalized to the measured integral of the deuteron current impinging on the target during the activation phase. Also, more precise estimates of the R^r and R^c were used that combine two corresponding up and down (u,d) detectors via the ratios r^r and r^c ("double ratio," Sec. V A). We obtain immediately the error ΔR of the corrected R coefficient

$$\Delta R=\frac{1}{1-I}\sqrt{(\Delta R^r)^2+I^2(J^b/J^r)^2(\Delta R^b)^2},$$

with

$$\Delta R^{r,b}=\frac{1}{J^{r,b}S}\,\frac{r^{r,b}}{(1+r^{r,b})^2}\sqrt{\sum_{\substack{i=u,+\\ j=d,-}}\frac{1}{N_j^{ir,b}}}.$$

The errors in the intensity ratio, I, and in the polarization of the target J, turned out to be negligible due to very high counting statistics.

The approach used in procedure (5) is different. Here, we subtract *the same* background contribution R^b from R^r values obtained for a few consecutive raw data files. Consequently, the corrected R coefficients are no more statistically independent. Typical values for the elements of the correlation matrix C [65] of the (*correlated*) results obtained after corrections of three consecutive raw data runs of 2 hours duration are

$$C=\begin{pmatrix}1.000 & 0.067 & 0.064\\ 0.067 & 1.000 & 0.061\\ 0.064 & 0.061 & 1.000\end{pmatrix}.$$

With the aid of the weight matrix $G=(g_{ij})$, which is the inverse of the covariance matrix [65], an estimator R of the expectation value of the R coefficient is determined by finding the maximum of the logarithm of the likelihood function $\mathscr{L}$:

$$\ln\mathscr{L}=\mathrm{const}+\sum_{i,j}\left[-\frac{1}{2}(R_i-R)g_{ij}(R_j-R)\right],$$

where the sums run over all corrected measurements. A maximum of the likelihood is obtained for

$$R=\sum_{i,j}g_{ij}\frac{1}{2}(R_i+R_j)\Big/\sum_{i,j}g_{ij}.$$

Additionally, we find that the error ΔR (at 68% C.L.) is given by

$$\Delta R=1\Big/\sqrt{\sum_{i,j}g_{ij}}$$

and that the quantity

$$\chi^2=\sum_{i,j}(R_i-R)g_{ij}(R_j-R)$$

plays the role of the conventional χ^2 that describes statistical consistency of the data set.

As an example, the results of the five analyses of the data acquired in series III of the measurements are presented in Table III. The foil-in R coefficients and the results *after* applying background correction are shown. Very good agreement between the corrected results for the five procedures of

TABLE IV. Raw R-correlation data (in 10^{-3}) and the *values* of corrections with their errors for all runs.

Run	I	II	III	IV
Raw data	12 ± 34	9 ± 12	-13 ± 7	-8 ± 4
Decay background	-39 ± 26	-13 ± 8	6 ± 4	0 ± 2
Gain shifts	-1 ± 3	-1 ± 2	-1 ± 1	-1 ± 1
Accidentals	-7 ± 8	-1 ± 2	2 ± 2	1 ± 1
β asymmetry	11 ± 5	13 ± 2	10 ± 1	6 ± 1
The result	-24 ± 44	7 ± 15	4 ± 8	-2 ± 5

the data analysis is observed. Consistency of the results was tested for all the procedures used in the data analysis by applying standard statistical tests. In Table III the values of $\chi^2/N_{\rm DF}$ and corresponding confidence levels are attached for the raw and corrected data. In all cases the statistical consistency of the data is significantly improved *after* applying the corrections with the resulting $\chi^2/N_{\rm DF}$ very close to one and high confidence levels.

The *measured asymmetries*, corresponding to the R-coefficient contributions shown in Table III, provide a somewhat better taste of the precision of the experiment. The weighted mean of all foil-in and foil-out asymmetries was $(-15\pm8)\times10^{-5}$ and $(-70\pm50)\times10^{-5}$, respectively. Although the latter error is by a factor of 6 larger than the former, the effective contribution of the background to the final uncertainty of the experiment is greatly reduced due to its low intensity I. The suppression factor is $I/(1-I)$, which results in our case in only half of the raw data error. This contribution, added in quadrature with the error of the foil-in data (statistical independence), increases the final error of the experiment only by 20%.

We note that the subtraction of the cosmic radiation and room background, that contribute at the level of ~0.001 of the events associated with the scattering from the analyzer foil, is included in the foil-out correction.

The background contribution has definitely the largest *uncertainty* of all applied corrections in this experiment. However, we stress that this uncertainty is determined solely by counting statistics in the measurements of the background radiation. In fact, the sequence 3/1 for the foil-in/foil-out measurements was chosen on the basis of pure statistical arguments to minimize the final error of the experiment.

2. β decay asymmetry

The false effect due to parity violation in β decay deserves truly the name ''systematic'': in contrast to the effects considered up to now, the correction and its uncertainty will not decrease with better statistics.

The discussion in Sec. IV C shows that the false effect grows rapidly with increasing acceptance angle of the analyzer foil. Therefore the width of the foil was decreased from 8 to 5 cm with increasing precision of the experiments (Table II), to reduce the value of this correction.

For each data taking run, we performed auxiliary measurements to determine the slope parameter ρ (Sec. IV C). In these measurements a 1 cm wide scattering foil was displaced from the median plane and the rate was measured as a function of the position h of the foil (Fig. 17). The up/down asymmetry in the rate, normalized to the rate observed with the foil placed in the median plane of the apparatus, provides the slope parameter $\rho=2.8\pm0.4$ that was used for the calculation of the false contribution $R=JA\alpha_0^2\rho/3$. The uncertainty quoted for this effect (Table IV) reflects the reproducibility of the measurements of the ρ parameter in various data collection runs.

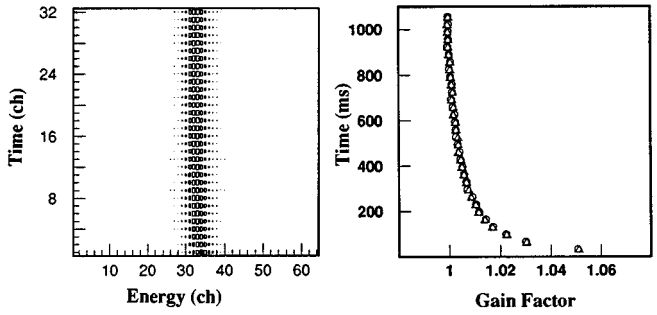

FIG. 20. Left: two dimensional spectrum of the light emitting diodes. Right: gain variation calculated from the centroids of LED's spectra for the $+/-$ spin states of the target (circles/triangles) as a function of time elapsed after activation. Gain is normalized to 1 at the end of the counting interval. Note expanded scale and virtually the same gain variations for the two spin states.

3. Small corrections and uncertainties

Gain shift. Before subtracting the foil-out background we applied corrections due to the gain shift of the photomultipliers. The 4 MeV analysis threshold is placed in the continuum of the energy spectrum (Fig. 14, Fig. 19), therefore gain variations of the detectors *in phase* with the polarization reversal are a potential source of a false asymmetry. The amplification of the detection system was monitored with light emitting diodes (LED), which fired well defined light pulses into the scintillators every millisecond during the 1 s long counting intervals. The energy spectra of the diodes were recorded for each E detector, in every 33 ms window following the target activation, and for $+/-$ spin states of the target separately. The centroids of the LED peaks are measured with great precision. Their positions were used to calculate the gain corrections. The observed larger amplifications, $\sim5\%$, at the beginning of the counting interval drop by a factor of 2 (Fig. 20) after ~100 ms.

Gain variations with their characteristic recovery time reflect sensitivities of the photomultipliers and the associated electronics to the total rate acquired during activation of the target. The observed rates were different by less than 1%. Therefore, amplification changes are very similar for the two polarization states of the ^{8}Li source. The ratio of the amplifications for $+$ and $-$ spin state is on the level 1.000 ± 0.001 for any time window after activation and for all the detectors used in our study. As a consequence, gain shift contributions to the asymmetries are strongly suppressed.

Gain correction was done file by file by fine adjustment of the lower integration limit in the energy$\times$time spectra for each detector, spin state, and time channel separately. Frac-

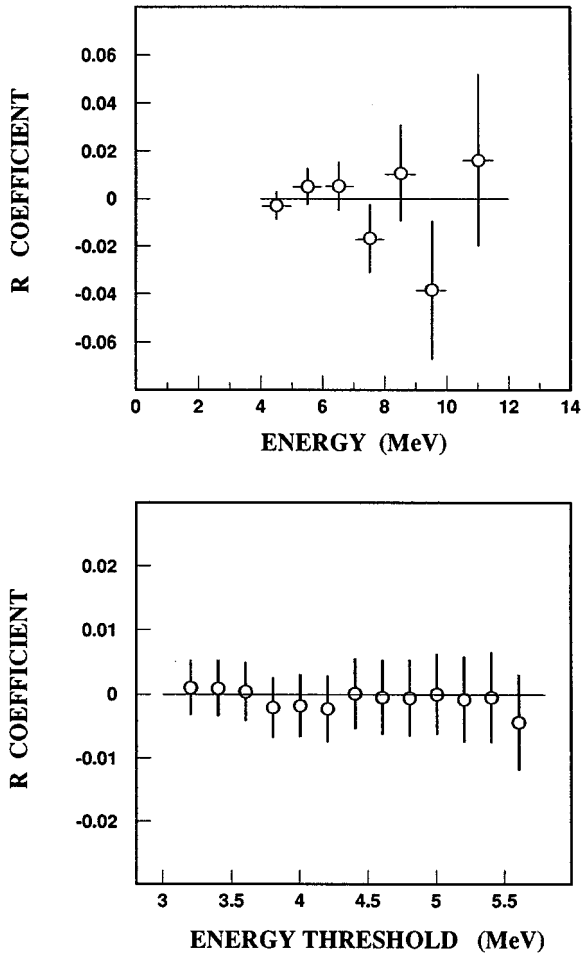

FIG. 21. Upper part: energy dependence of the R coefficient determined in this experiment. Lower part: dependence of the result on the threshold assumed in the data analysis (run IV with the highest statistics). Note that the data points in the lower figure are *not* statistically independent.

tional contents of the channel corresponding to the 4 MeV energy threshold were used in the calculation. The resulting average correction to the R coefficient due to gain shifts is $-(1\pm1)\times10^{-3}$. The error is calculated from the dispersion of all gain corrections.

Accidental coincidences. One of the reasons to use triple detector telescopes was suppression of random events. They were measured by inserting delay lines before forming fast coincidences for each telescope. The measurements were performed with the scattering foil in place and the foil removed. The intensity of accidentals was only ~0.0007 of the foil scattered events (Fig. 14, Fig. 19). For example, in the III run the asymmetries of the accidental coincidences, averaged over all detectors, were -0.05 ± 0.02 (foil in) and -0.03 ± 0.03 (foil out). These numbers might indicate an asymmetry that is consistent with the value -0.029 ± 0.001, measured by the target polarization monitors. We hypothesize therefore that accidental coincidences are caused by radiation uncorrelated in time, which penetrates through the passive shielding into δ, Δ, and E detectors.

Accidental coincidences were subtracted in the same manner as the background radiation discussed in Sec. V D.

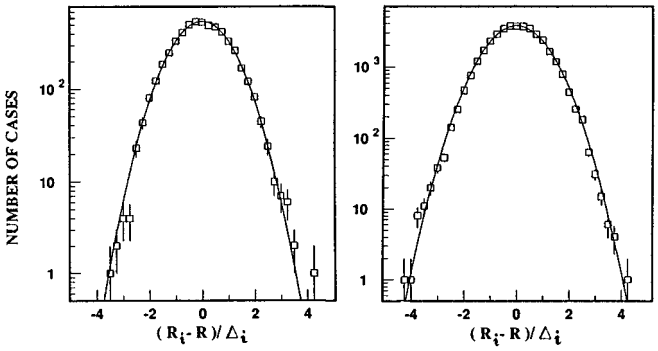

FIG. 22. Distribution of the deviations of the R_i coefficients from their mean R, normalized to the errors ΔR_i. Left: analysis (3); right: analysis (4). Solid lines show Gaussian distributions with unit variance, centered at the origin.

Only integrated effects were evaluated since in most channels of the fine time$\times$energy grid no counts were observed. Attention was paid to avoid double subtraction, since a great part of the random events was already taken into account in the foil-out corrections. Therefore, the effects associated with the foil-in accidentals were added, and the foil-out corrections were subtracted. The error of the accidental coincidences is once again determined by counting statistics.

Electronic effects. The electronics used in this experiment was set up to reduce spurious asymmetries due to dead time and pile up effects to a level negligible compared with the uncertainty of the raw data. False effects from dead time of the analog-to-digital converters (ADC) were eliminated by gating all ADC's with mixed pulses from all the detectors (common gate principle). This equalizes the dead time correction factors for corresponding up and down detectors. Consequently, the ''double ratio'' (Sec. V A) that was used to calculate asymmetries is not influenced by dead time losses. The estimated losses in fast discriminators due to pile up of the incoming pulses could result in asymmetries that are two orders of magnitude lower than the statistical uncertainty of the final result.

VI. RESULTS

A. Final data and tests

The final results for all the runs are shown in Table IV. We have checked that the various methods of data analysis lead to results that are consistent at the level of $\sim1/10$ of the final error bar (Table III). The dominant contribution to the final error of the experiment comes from the counting statistics in the measurements with the scattering foil in place and the foil removed (Table III, Table IV).

An energy measurement in this experiment was conceived to examine the energy dependence of the R coefficient. The motivation here was not to detect an effect (first of all one would expect a nonzero *average* R correlation), but rather to check the consistency of the results. In fact, no such dependence is seen and our result is also stable as a function of the threshold assumed in the analysis (Fig. 21).

We have examined the distributions of the corrected results for the analysis procedures with a large number of degrees of freedom. Since the errors ΔR_i of the independent

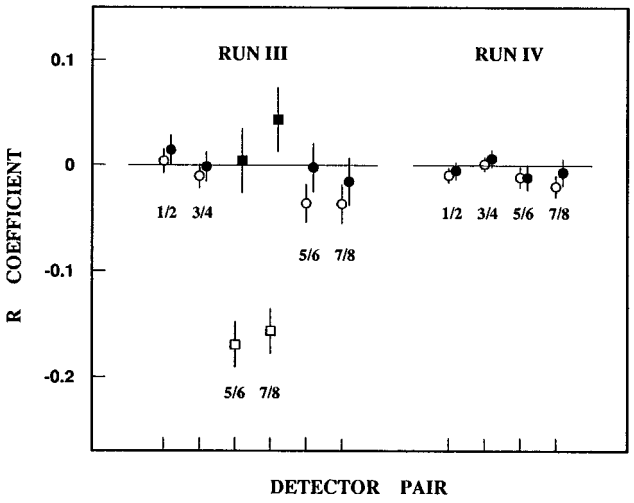

FIG. 23. R coefficients for runs III and IV, obtained from raw data (open symbols) and after applying all corrections (filled symbols). The detector pairs are indicated. Dots: well shielded detectors, low background conditions. Squares: data taken with high background due to incomplete shielding of new detectors installed at the beginning of the run III (pairs 5/6 and 7/8, Fig. 10). Note the decrease of the corrections for the pairs 5/6 and 7/8 after inserting additional shielding during the run III and consistency of all corrected data with the final result of this experiment (solid line).

R-coefficients R_i that contribute to the mean value R are vastly different, a standardized random variable $(R_i-R)/\Delta R_i$ was investigated. This variable should have a normal distribution with a central value at zero and a standard deviation equal to one. Figure 22 shows the excellent agreement of the data with these expectations.

Beside positive results of the statistical tests we also have more direct evidence that the corrections were calculated with sufficient precision. At the beginning of the run III we realized that the raw data for the new mounted detectors exhibited an unexpectedly large asymmetry that was clearly incompatible with all our previous results. The cause was imperfect shielding of the light guides for the Δ counters in the new segments of the apparatus. A lightguide area of only few cm^2 was exposed to the electrons emitted directly from the ^{8}Li source. It turned out that the Cerenkov light produced in the thick part of the lightguides strongly increased the intensity and the asymmetry of the foil-out background and the level of the accidental coincidences. After insertion of additional shielding the raw data from the new detectors did not exhibit any anomaly.

Without shields, we observed an ~ 7 standard deviation signal simulating time reversal violation in the foil-in data. However, after applying our standard procedures, the corrected results are consistent with all the other data (Fig. 23). From this agreement we conclude therefore that the overall corrections in this experiment are calculated with required precision.

Some apparent inconsistency (Table IV) in the background correction for different runs requires a brief comment. Variations in the value of this correction are not surprising, since the detectors in the following runs operated in different background conditions (one quarter, one half, and the whole apparatus assembled). Obviously, this correction is particularly sensitive to the configuration of the shielding of the detectors, which was greatly altered from run to run.

Although the correction due to β decay asymmetry is the largest one, it is known so precisely that its *uncertainty* is almost negligible. One notes that the effect due to β decay asymmetry for the first data collection run is somewhat smaller, in spite of using the widest (8 cm) analyzer foil. This is due to a different positioning of the detectors in the prototype apparatus than in the following runs, and a $\sim 10\%$ larger distance between the ^{8}Li source and the lead foil. After analysis of the first data we concluded that the effects due to β decay asymmetry can be measured quite precisely. We allowed therefore slightly larger values for this correction by redesigning the apparatus. These alterations increased the statistical sensitivity of the experiment. The fake β asymmetry effect scales correctly with the height of the scattering foil in the last three runs.

B. Result for R parameter

By averaging all the acquired data we obtain the value of the triple correlation coefficient R between the nuclear spin $\vec{J}$, the momentum of the electron $\vec{p}$, and the spin $\vec{\sigma}$ of the electron emitted in ^{8}Li decay:

$$R=(-0.2\pm 4.0)\times 10^{-3}.$$

This is the most precise determination of the transverse polarization of leptons emitted in weak decays.

VII. DISCUSSION

A. Formalism

In general, the R correlation for the mixed Fermi/Gamow-Teller transition bears information on the combination of the strengths of time reversal violating parts of the weak *scalar* and *tensor* interaction. For transitions between nuclear levels with the same spin I and parity π (all cases considered in this section), the explicit expression for the R parameter is [50]

$$\begin{aligned} R\xi = R_{\mathrm{FSI}}\xi &+ |M_{\mathrm{GT}}|^2 \frac{1}{I+1} 2\,\mathrm{Im}(C_T C_A'^* + C_T' C_A^*) \\ &+ M_F M_{\mathrm{GT}} \sqrt{\frac{I}{I+1}} 2\,\mathrm{Im}(C_S C_A'^* + C_S' C_A^* \\ &- C_V C_T'^* - C_V' C_T^*), \end{aligned}$$

with

$$\begin{aligned} \xi = &|M_F|^2(|C_S|^2+|C_V|^2|+|C_S'|^2+|C_V'|^2) \\ &+|M_{\mathrm{GT}}|^2(|C_T|^2+|C_A|^2|+|C_T'|^2+|C_A'|^2). \end{aligned}$$

The contribution R_{FSI}, due to the electromagnetic interaction of the electron in the final state with a point nucleus, has the form [50]

$$R_{\mathrm{FSI}}\xi = -\frac{\alpha Z m}{p}\Bigg[|M_{\mathrm{GT}}|^2\frac{1}{I+1}2\,\mathrm{Re}(C_T C_T'^{*} - C_A C_A'^{*}) + M_F M_{\mathrm{GT}}\sqrt{\frac{I}{I+1}}2\,\mathrm{Re}(C_S C_T'^{*} + C_S' C_T^{*} - C_V C_A'^{*} - C_V' C_A^{*})\Bigg].$$

Here, the matrix elements M_F, M_{GT} take into account the structure of the nuclear states involved in the transition, while the coupling constants C_V, C_A, ... describe effects of the weak interaction arising from the vector (V), axial vector (A), scalar (S), and tensor (T) variants of the theory [44]; α is the fine structure constant and m,p are the electron mass and momentum, respectively. Fortunately, the procedure used to obtain effective matrix elements " ... presents no fundamental difficulties for nuclear β-decay experiments discussed below ... " [66].

Recently a new parametrization [66,67] of the β decay Hamiltonian based on the helicity projection (HP) formalism has been introduced. In this formalism the handeness (L-left, and R-right) of the initial quark (q) and the charged lepton l involved in the four fermion point interaction is explicitly displayed. The expressions for the $A,R,D,\ldots$ observables in the HP form are lengthy, therefore we list only the relations between the coupling constants C_i, C_i' and the HP amplitudes a_{lq}^i ($i=V,A,S,T$, $l=L,R$, $q=L,R$):

$$C_V = g_V(a_{LL}^V + a_{LR}^V + a_{RL}^V + a_{RR}^V),$$

$$C_V' = g_V(a_{LL}^V + a_{LR}^V - a_{RL}^V - a_{RR}^V),$$

$$C_A = -g_A(a_{LL}^V - a_{LR}^V - a_{RL}^V + a_{RR}^V),$$

$$C_A' = -g_A(a_{LL}^V - a_{LR}^V + a_{RL}^V - a_{RR}^V),$$

$$C_S = g_S(a_{LL}^S + a_{LR}^S + a_{RL}^S + a_{RR}^S),$$

$$C_S' = -g_S(a_{LL}^S + a_{LR}^S - a_{RL}^S - a_{RR}^S),$$

$$C_T = 2g_T(a_{LR}^T + a_{RL}^T),$$

$$C_T' = -2g_T(a_{LR}^T - a_{RL}^T).$$

The standard model assumes that $a_{LL}^V = 1$ and all other a_{ql}^i amplitudes vanish. The form factors g_i correspond to the transition from the description of fundamental β decay processes on the level of quarks to nucleons. The values of the vector g_V and axial vector g_A form factors, obtained from the β decay of a free neutron, are 1 and 1.26, respectively. Since no such experimental data on g_S and g_T are available, we must use theoretical estimates; e.g., the simplest quark model or the bag model of a nucleon predict $g_S \simeq 0.5$ and $g_T \simeq 1.4$[68], with estimated uncertainties about 30%.

B. Time reversal symmetry in ^{8}Li decay

The $^8\mathrm{Li} \rightarrow {}^8\mathrm{Be}$ transition occurs between the $I^\pi = 2^+$, $T=1$ and $I^\pi = 2^+$, $T=0$ levels (Fig. 1), and due to the isospin, T, selection rule it is dominated by the Gamow-Teller strength. The likely Fermi admixture is in the order of $|M_F/M_{\mathrm{GT}}|^2 \sim 0.001$ only [52]. Therefore, contribution from the Fermi/Gamow-Teller interference term to the R correlation may be safely neglected for the ^{8}Li decay.

The effects of the final state interaction, which can mimic genuine time reversal violation in the R correlation, are exceptionally small for the ^{8}Li decay (Sec. III). An average value of the FSI correction in the point nucleus approximation, weighted by the energy spectrum of the scattered electrons with $E > 4$ MeV, amounts to $R_{\mathrm{FSI}} = 0.7 \times 10^{-3}$. More subtle contributions to the FSI correction were investigated in Ref. [69], where it was shown that, e.g., the effects of the finite nuclear size influence the result by less than 10%. False time reversal violation effects due to the two α particles which are decay products of the residual ^{8}Be nucleus are negligible at the present experimental accuracy. The insensitivity of the R observable to the strong interaction phase shifts in the final state results from the fact that the two α particles are not detected in this experiment. Recently, very detailed calculations [70] show that the strong interaction induced FSI effects in the $A=8$ system are much smaller than the electron-nucleus Coulomb interaction ones and there is a strong cancellation between several second forbidden terms in the region of the 2^+ state of the residual nucleus (Fig. 1). We conclude, therefore, that the first order approximation for the FSI correction [50] is adequate in our case.

Taking into account the FSI effects we obtain the result for the time reversal violating part R_{TRV} of the R correlation:

$$R_{\mathrm{TRV}} = (-0.9 \pm 4.0) \times 10^{-3}.$$

This result is consistent with time reversal invariance.

C. Limits for tensor interaction

Ignoring isospin impurities and Fermi/Gamow-Teller interference, the largest contribution to R_{TRV} in our experiment comes from the axial vector–tensor term:

$$R_{\mathrm{TRV}} = \frac{2}{3}\frac{\mathrm{Im}(C_T C_A'^{*} + C_T' C_A^{*})}{|C_A|^2 + |C_A'|^2} \approx \mathrm{Im}\left(\frac{C_T + C_T'}{3C_A}\right),$$

where the approximation is valid for $C_A = C_A'$.

Using the same approximation, the R coefficient for ^{8}Li decay may be expressed in the helicity projection formalism as

$$R_{\mathrm{TRV}} = -\frac{4}{3}\mathrm{Im}\left(\frac{g_T}{g_A}a_{RL}^T\right).$$

Our result provides new 1σ limits on the imaginary parts of the tensor couplings in semileptonic, strangeness conserving weak decays:

$$-0.015 < \mathrm{Im}\left(\frac{C_T + C_T'}{C_A}\right) < 0.009$$

$$-0.002 < \mathrm{Im}(a_{RL}^T) < 0.003.$$

Alternatively, the 90% C.L. limits are

$$-0.022<\mathrm{Im}\left(\frac{C_T+C_T'}{C_A}\right)<0.017$$

$$-0.004<\mathrm{Im}(a_{RL}^T)<0.005.$$

D. Analysis of T violation in β decay

β decay experiments, which examine the *first order* (i.e., *linear* in the decay amplitude) time reversal violation arising from physics beyond the standard *V-A* approach, are in general sensitive to a linear combination of the two exotic, i.e., scalar and tensor interaction terms. Available data may be therefore conveniently presented as exclusion plots in the plane defined by the two components of the weak interaction:

$$S=\mathrm{Im}[(C_S+C_S')/C_A],\ T=\mathrm{Im}[(C_T+C_T')/C_A].$$

The experiment reported in this work is sensitive solely to the T contribution and measures limits of $-0.015<T<0.009$. Earlier 1σ limits $-0.073<T<-0.007$ [71] have been derived from the subtle final state interaction corrections to the longitudinal electron polarization in the decay of ^{153}Sm. We note that the data [72] analyzed in Ref. [71] were not taken with the intention to investigate time reversal violation phenomena. In addition, the indirect determination [71] depends critically on the assumptions which had to be made in the analysis (highly hindered GT transition, constraints on the values of the other coupling constants, etc.). Recent reviews [66] comment " ... the (^{153}Sm) FSI result should not be taken too seriously ... " since " ... these estimates are deemed unreliable, especially for hindered transitions ... . " Since our experiment provides direct and much tighter constraints for the time reversal violating tensor terms, the ^{153}Sm estimation and associated ambiguities do not have to be considered any more.

The only other R-type measurement, with ^{19}Ne (Table I), is more sensitive to scalar interaction. Accordingly, the authors [38] have chosen to analyze $\mathrm{Im}(C_S)$. Neglecting the tensor contribution they obtain the result equivalent to $0.077<S<0.410$. In our reanalysis of the ^{19}Ne R experiment in terms of the linear combination, assuming that the nuclear matrix elements are $M_F=1$ and $M_{\mathrm{GT}}=-1.28$[38], and $C_A=C_A'=-1.26$, we obtain

$$R(^{19}\mathrm{Ne})=-0.33S-0.22T.$$

A recent paper [73] presents a new idea of using the electron-neutrino angular correlation a [50] in a pure Fermi transition as a probe of the scalar couplings. This observable provides limits for the absolute values of the couplings $|C_S|$, $|C_S'|$. These limits also restrict the imaginary part of the scalar interaction. An analysis [73] of the β delayed proton spectroscopy study of ^{32}Ar and ^{33}Ar decays [74] yields $|C_S|/|C_V|<0.167$ and $|C_S'|/|C_V|<0.167$ (2σ constraints). Scaling these results to 1σ limits for the sake of comparison with the other experiments, and combining the two contributions in quadrature, we obtain $S=0.000\pm0.094$. The method of Ref. [73] was also applied in the case of the pure Gamow-Teller decay of ^{6}He [75], to restrict β decay tensor couplings $|C_T|/|C_V|$ and $|C_T'|/|C_V|$ on the 1σ level, to values less than 0.121 [76]. However, this determination, interpreted in terms of the considered combination T of the time reversal violating couplings, is much less precise than the result from the experiment discussed in this work.

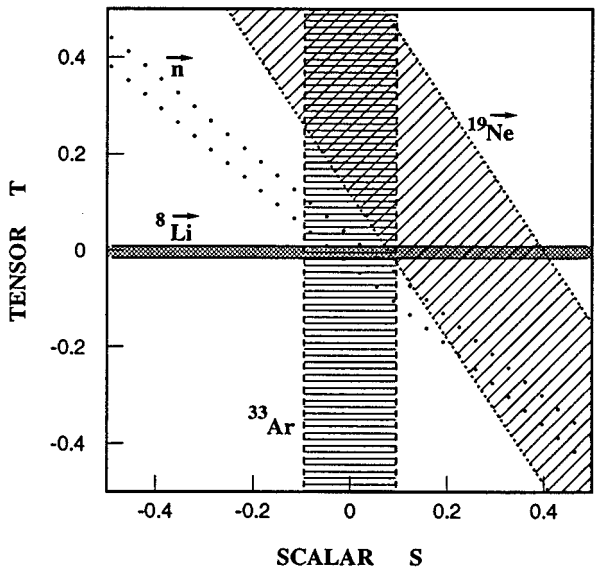

FIG. 24. Results from the most precise, recent experiments testing time reversal symmetry in the scalar and tensor weak interactions. The bands indicate $\pm1\sigma$ limits from the measurements reported in Refs. [38,74,73] and in this work. Constraints from the R-correlation experiment in the decay of free neutrons, to be measured with an accuracy of ±0.01, are attached.

Figure 24 sumarizes the restrictions available from the most sensitive β decay experiments searching for time reversal violation in scalar and tensor weak interactions.

Although consistency between all the relevant measurements is far from ideal, a fair conclusion is that no evidence of time reversal violation can be inferred from β decay data.

VIII. SUMMARY

This study represents a first direct measurement of the triple angular correlation R for a β decay transition, which is sensitive to the time reversal violating, charge changing weak tensor amplitude. We reiterate [8,66,67] that, in contrast to common opinions, such interaction terms may be present in gauge invariant, renormalizable extensions of the standard model.

The present study has improved by almost an order of magnitude our knowledge of this part of the time reversal violating weak interaction, which also violates parity symmetry (Table I). As a result, T-violating, charge changing tensor couplings are determined directly with much better precision than the other exotic term, the scalar weak interaction.

In the next step, a comparable improvement in the scalar sector would be welcomed. An experiment with Ar nuclei is in preparation to achieve this goal [77]. This experiment aims at a determination of the magnitude of the scalar couplings by measuring the squares of the weak amplitudes, and therefore is not sensitive in the first order to the time reversal violating part S. Here, the expected one order of magnitude

improvement in the experimental accuracy of the electron-neutrino correlation will bring a factor of ~ 3 in the amplitude S.

Past experience from the precision studies of parity and time reversal symmetries shows that redundancy in these difficult measurements is desirable. There are two candidate systems which possess important advantages (which will not be discussed here) for a first order measurement of T violation arising via scalar couplings. One of them, which has already produced the first R-correlation results [38], is being considered for an upgrade at Princeton University [38,78]. Atomic physics methods based on lasers are proposed, in order to polarize the ^{19}Ne nuclei, and to achieve an order of magnitude improvement in the accuracy. The other case is even more interesting. According to our estimations, an experiment to determine transverse polarization of electrons emitted in the decay of polarized free neutrons is feasible on the level of ± 0.01 in the R-correlation coefficient. The expected constraints are presented in Fig. 24. Although this experiment provides similar information to that from ^{19}Ne decay, it has the additional advantage of studying a particularly simple system, which serves as a basic laboratory for weak interactions in semileptonic decays.

ACKNOWLEDGMENTS

The authors wish to thank Dr. P. Schmelzbach, Dr. H. Einenkel, and the operating staff of the PSI accelerators for providing excellent beams for this experiment. We thank H. Blumer and B. Zimmermann from the PSI Workshop and W. Gruber for their help in the construction of the apparatus. Financial support of PSI, Swiss National Foundation and United States National Science Foundation is gratefully acknowledged.

[1] G. Lüders, Dansk. Mat. Fys. Medd. **28**, 5 (1954); W. Pauli, in *Niels Bohr and the Development of Physics*, edited by W. Pauli (Pergamon Press, New York, 1955), p. 30.
[2] Particle Data Group, Phys. Rev. D **50**, 1175 (1994); L.K. Gibbons *et al.*, Phys. Rev. Lett. **70**, 1199 (1993).
[3] L. Wolfenstein, Phys. Rev. Lett. **13**, 562 (1964).
[4] M. Kobayashi and K. Maskawa, Prog. Theor. Phys. **49**, 652 (1972); N. Cabibbo, Phys. Rev. Lett. **10**, 531 (1963).
[5] G. 't Hooft, Phys. Rev. Lett. **37**, 8 (1976).
[6] R.N. Mohapatra and J.C. Pati, Phys. Rev. D **11**, 566 (1975).
[7] S. Weinberg, Phys. Rev. Lett. **36**, 657 (1976); T.D. Lee, Phys. Rev. D **8**, 1226 (1973); Phys. Rep. **96**, 143 (1979).
[8] W. Buchmüller, R. Rückl, and D. Wyler, Phys. Lett. B **191**, 442 (1987); W. Buchmüller and D. Wyler, *ibid.* **177**, 377 (1986); P. Herczeg, in *Fundamental Symmetries in Nuclei and Particles*, edited by H. Henrikson and P. Vogel (World Scientific, Singapore, 1989), p. 46.
[9] S. Weinberg, in *The First Three Minutes* (Basic Books Inc., New York, 1977); Phys. Rev. Lett. **42**, 850 (1979).
[10] A.D. Sakharov, JETP Lett. **5**, 24 (1967).
[11] P. Langacker, in *CP Violation*, edited by C. Jarlskog, Advanced Series on Directions in High Energy Physics Vol. 3 (World Scientific, Singapore, 1989), p. 552; A.G. Cohen, D. B. Kaplan, and A.E. Nelson, Annu. Rev. Nucl. Part. Sci. **43**, 27 (1993) and references therein.
[12] J.H. Christenson, J.W. Cronin, V.L. Fitch, and R. Turlay, Phys. Rev. Lett. **13**, 138 (1964); see also references in [2].
[13] K. Kleinknecht, Comments Nucl. Part. Phys. **18**, 291 (1989) and references therein.
[14] L.K. Gibbons *et al.*, Phys. Rev. Lett. **70**, 1203 (1993); L. Iconomidou-Fayard *et al.*, in *Tests of Fundamental Symmetries*, XXVIth Rencontre de Moriond, edited by O. Fackler, G. Fontaine, and J. Tran Thanh Van (Editions Frontiers, Singapore, 1991), Vol. M68, p. 321; K. Kleinknecht, Comments Nucl. Part. Phys. **20**, 281 (1992).
[15] H. Burkhardt *et al.*, Phys. Lett. B **206**, 169 (1988).
[16] E.J. Ramberg *et al.*, Phys. Rev. Lett. **70**, 2529 (1993).
[17] E.D. Commins and P.H. Bucksbaum, *Weak Interactions of Leptons and Quarks* (Cambridge University Press, Cambridge, England, 1983), p. 270.
[18] R. Adler *et al.*, Phys. Lett. B **286**, 180 (1992); R. Adler *et al.*, in *Particles and Nuclei*, XIIIth International Conference, Perugia, Italy, 1993, edited by A. Pascolini (World Scientific, Singapore, 1994), p. 273.
[19] G. Buchalla, A.J. Buras, and M.K. Harlander, Nucl. Phys. **B349**, 1 (1991).
[20] The BaBar Collaboration, ''Letter of Intent for the Study of *CP* Violation and Heavy Flavor Physics at PEP-II,'' SLAC Report 443, June 1994; similar project was recently approved at KEK, Tsukuba.
[21] B. Winstein, Phys. Rev. Lett. **68**, 1271 (1992).
[22] W.J. Marciano, in *BNL Study on CP Violation*, edited by S. Dawson and A. Soni (World Scientific, Singapore, 1991), p. 35.
[23] E.P. Shabalin, Sov. J. Nucl. Phys. **28**, 75 (1978).
[24] K.F. Smith *et al.*, Phys. Lett. B **234**, 191 (1990); I.S. Altarev *et al.*, *ibid.* **276**, 242 (1992); J.P. Jacobs *et al.*, Phys. Rev. Lett. **71**, 3782 (1994); K. Abdullach *et al.*, *ibid.* **65**, 2347 (1990).
[25] N.F. Ramsey, Annu. Rev. Nucl. Part. Sci. **40**, 1 (1990).
[26] Review of the experiments and theoretical predictions: J.M. Pendelbury, Annu. Rev. Nucl. Part. Sci. **43**, 687 (1993).
[27] A. Bohr and B. Mottelson, in *Nuclear Structure, Vol. 1* (W.A. Benjamin Inc., New York, 1969).
[28] E. Blanke *et al.*, Phys. Rev. Lett. **51**, 355 (1983).
[29] T.S. Bhatia *et al.*, Phys. Rev. Lett. **48**, 227 (1982); R.A. Hardekopf *et al.*, Phys. Rev. C **25**, 1090 (1982).
[30] V.E. Bunakov, Phys. Rev. Lett. **60**, 2250 (1988); J.D. Bowman, in *Intersections Between Particle and Nuclear Physics*, edited by D.F. Geesaman, AIP Conf. Proc. No. 150 (AIP, New York, 1986), p. 1194; Y. Masuda and S. Seestrom, in Tests of Fundamental Laws, XXXth Rencontre de Moriond, Villars, Switzerland, 1995 (unpublished).
[31] J.L. Gimlett *et al.*, Phys. Rev. C **25**, 1567 (1980); J.L. Gimlett *et al.*, Phys. Rev. Lett. **42**, 354 (1979); N.K. Cheung *et al.*, Phys. Rev. C **16**, 2381 (1977).
[32] R.I. Steinberg *et al.*, Phys. Rev. Lett. **33**, 41 (1974); R.I. Steinberg *et al.*, Phys. Rev. D **13**, 2469 (1976).
[33] B.G. Erozolimsky, JETP Lett. **20**, 345 (1974).
[34] M. Baltrusaitis *et al.*, Phys. Rev. Lett. **38**, 464 (1977). A.L.

Hallin *et al.*, *ibid.* **52**, 337 (1984).
[35] M.K. Campbell *et al.*, Phys. Rev. Lett. **47**, 1032 (1981).
[36] W.M. Morse *et al.*, Phys. Rev. D **21**, 1750 (1980).
[37] S.Y. Hsueh *et al.*, Phys. Rev. D **38**, 2056 (1988).
[38] M.B. Schneider *et al.*, Phys. Rev. Lett. **51**, 1239 (1983).
[39] C.E. Overseth and R.F. Roth, Phys. Rev. Lett. **19**, 391 (1967).
[40] W.E. Cleland *et al.*, Nucl. Phys. **B40**, 221 (1972).
[41] H. Burkard *et al.*, Phys. Lett. **160B**, 343 (1985).
[42] T.J. Bowles, in *Tests of Time Reversal Invariance in Neutron Physics*, edited by N.R. Roberson, C.R. Gould, and J.D. Bowman (World Scientific, Singapore, 1987), p. 71; G. Greene (personal communication); J. Imazato *et al.*, KEK-PS Research Proposal, Tsukuba, 1991.
[43] R.P. Feynman and M. Gell-Mann, Phys. Rev. **109**, 193 (1958).
[44] C.S. Wu and S. A. Moszkowski in *Beta Decay* (John Wiley, New York, 1966); F. Scheck, in *Leptons, Hadrons and Nuclei* (North-Holland Physics Publishing, Amsterdam, 1983); C. Itzykson and J.P. Zuber, in *Quantum Field Theory* (McGraw-Hill Book Co., New York, 1980).
[45] E.G. Adelberger, Phys. Rev. Lett. **70**, 2856 (1993); A.I. Boothroyd, J. Markey, and P. Vogel, Phys. Rev. C **29**, 603 (1984).
[46] V. N. Bolotov, Phys. Lett. B **243**, 308 (1990); A.A. Poblaguev, *ibid.* **238**, 108 (1990).
[47] M.B. Voloshin, Phys. Lett. B **283**, 120 (1992); A.A. Poblaguev, *ibid.* **286**, 169 (1992); P. Quin *et al.*, Phys. Rev. D **47**, 1247 (1993).
[48] M. Allet *et al.*, Phys. Rev. Lett. **68**, 572 (1992).
[49] T.D. Lee and C.N. Yang, Phys. Rev. **104**, 254 (1956).
[50] J.D. Jackson, S.B. Treiman, and H.W. Wyld, Phys. Rev. **106**, 517 (1957); Nucl. Phys. **4**, 206 (1957).
[51] F. Ajzenberg Selove, Nucl. Phys. **A490**, 1 (1988).
[52] R.E. Tribble and G.T. Garvey, Phys. Rev. C **12**, 967 (1975).
[53] J. Liechti, Dissertation No. 8786, ETH Zürich, 1989; Z. Wang *et al.*, Phys. Rev. C **40**, 1586 (1989).
[54] J.R. Hall, Dissertation, Stanford Univ., 1982.
[55] J.R. Hall *et al.*, Nucl. Phys. **A483**, 1 (1988); R.A. Bigelow, Dissertation, University of Wisconsin, 1986.
[56] F. Fujara *et al.*, Z. Phys. **B37**, 151 (1980); H. Ackermann *et al.*, Hyperfine Interact. **24-26**, 395 (1985).
[57] N. Sherman, Phys. Rev. **103**, 1601 (1956); P. Ugincius *et al.*, Nucl. Phys. **A158**, 418 (1970); J. Kessler, in *Polarized Electrons* (Springer-Verlag, Berlin, 1976).
[58] H. Lüscher, Dissertation No. 9507, ETH Zürich, 1991.
[59] V. Spiegel *et al.*, Ann. Phys. (N.Y.) **6**, 70 (1959).
[60] H. Wegener, Z. Phys. **151**, 252 (1958).
[61] A.R. Brossi *et al.*, Nucl. Phys. **33**, 353 (1962).
[62] D. Conti, Diploma, ETH Zürich, 1994; D. Conti *et al.*, Helv. Phys. Acta **67**, 777 (1994).
[63] B. Blake and B. Mühlschlegel, Z. Phys. **167**, 584 (1962).
[64] J. Sromicki *et al.*, 7th International Conference on Polarization Phenomena in Nuclear Physics, Paris, June 1990 [J. Phys. (Paris) Colloq. **51**, C6-527 (1990)]; M. Allet *et al.*, *Proceedings of the 9th International Symposium on High Energy Spin Physics*, Bonn, 1990 (Springer-Verlag, Berlin, 1990), p. 585; M. Allet *et al.*, in *Tests of Fundamental Symmetries*, XXVIth Rencontre de Moriond, edited by J. Tran Thanh Van (Editions Frontiers, Singapore, 1991), Vol. M68, p. 30; M. Allet *et al.*, *Intersections Between Particle and Nuclear Physics*, Tucson, AZ, 1991, AIP Conf. Proc. No. 243 (AIP, New York, 1991), p. 977; M. Allet *et al.*, in *Tests of Fundamental Symmetries*, XIIth Rencontre de Moriond, edited by J. Tran Thanh Van (Editions Frontiers, Singapore, 1992), Vol. M72, p. 299; M. Allet *et al.*, in *10th International Symposium on High Energy Spin Physics*, Nagoya, Japan, 1992 (Universal Academy Press Inc., Tokyo, 1993), p. 753.
[65] S. Brandt, in *Statistical and Computational Methods in Data Analysis* (North-Holland, Amsterdam, 1976).
[66] J. Deutsch and P. Quin, in *Precision Tests of the Standard Electroweak Model*, edited by P. Langacker (World Scientific, Singapore, 1993); P. Quin, Nucl. Phys. **A553**, 319c (1993).
[67] P. Herczeg, in *Precision Tests of the Standard Electroweak Model*, edited by P. Langacker (World Scientific, Singapore, 1993).
[68] S.L. Adler *et al.*, Phys. Rev. D **11**, 3309 (1975).
[69] P. Vogel and B. Werner, Nucl. Phys. **A404**, 345 (1983).
[70] S. Ying and E.M. Henley, Nucl. Phys. **A585**, 463 (1995).
[71] M. Skalsey and M.S. Hatamian, Phys. Rev. C **31**, 2218 (1985).
[72] J. van Klinken, Nucl. Phys. **75**, 145 (1966).
[73] E.G. Adelberger, Phys. Rev. Lett. **70**, 2856 (1993).
[74] D. Schardt and K. Riisager, Z. Phys. **A345**, 265 (1993).
[75] C.H. Johnson, F. Pleasonton, and T.A. Carlson, Phys. Rev. **132**, 1149 (1963).
[76] M. Skalsey, Phys. Rev. C **49**, R620 (1994).
[77] E.G. Adelberger *et al.*, IS 334, CERN proposal at ISOLDE.
[78] A. Young, International Workshop on Symmetry Tests, Louvain-la-Neuve, June 1993 (unpublished).